The Meteoritical Society

Meteoritics & Planetary Science 49, Nr 6, 958–977 (2014)
doi: 10.1111/maps.12307

Magnetic properties of the LL5 ordinary chondrite Chelyabinsk (fall of February 15, 2013)

Natalia S. BEZAEVA[1,2*], Dmitry D. BADYUKOV[3], Mikhail A. NAZAROV[3], Pierre ROCHETTE[4], Joshua M. FEINBERG[5,6], Gennadiy P. MARKOV[7], Daniel BORSCHNECK[4], François DEMORY[4], Jérôme GATTACCECA[4,8], Sergey E. BORISOVSKIY[9], and Anna Ya SKRIPNIK[3]

[1]Earth Physics Department, Faculty of Physics, M.V. Lomonosov Moscow State University, Leninskie Gory, 119991 Moscow, Russia
[2]Ural Federal University, 19 Mira Str., 620002 Ekaterinburg, Russia
[3]Vernadsky Institute of Geochemistry and Analytical Chemistry, Russian Academy of Sciences, 19 Kosygin Str., 119991 Moscow, Russia
[4]CEREGE CNRS/Aix-Marseille Université, BP 80, 13545 Aix en Provence, Cedex 4, France
[5]Institute for Rock Magnetism, University of Minnesota, 100 Union Drive SE, Minneapolis, Minnesota 55455, USA
[6]Department of Earth Sciences, University of Minnesota, 310 Pillsbury Drive SE, Minneapolis, Minnesota 55455, USA
[7]Schmidt Institute of Physics of the Earth, Russian Academy of Sciences, B. Gruzinskaya Str., 123995 Moscow, Russia
[8]Department of Earth, Atmospheric, and Planetary Sciences, Massachusetts Institute of Technology, 77 Massachusetts Avenue, Cambridge, Massachusetts 02139, USA
[9]Institute of Geology of Ore Deposits, Petrography, Mineralogy and Geochemistry, Russian Academy of Sciences, 35 Staromonetny Per., 119017 Moscow, Russia
[*]Corresponding author. E-mail: bezaeva@physics.msu.ru

(Received 24 September 2013; revision accepted 06 April 2014)

Abstract–Here we characterize the magnetic properties of the Chelyabinsk chondrite (LL5, S4, W0) and constrain the composition, concentration, grain size distribution, and mineral fabric of the meteorite's magnetic mineral assemblage. Data were collected from 10 to 1073 K and include measurements of low-field magnetic susceptibility (χ_0), the anisotropy of χ_0, hysteresis loops, first-order reversal curves, Mössbauer spectroscopy, and X-ray microtomography. The REM and REM′ paleointensity protocols suggest that the only magnetizations recorded by the chondrite are components of the Earth's magnetic field acquired during entry into our planet's atmosphere. The Chelyabinsk chondrite consists of light and dark lithologies. Fragments of the light lithology show $\log\chi_0 = 4.57 \pm 0.09$ (s.d.) ($n = 135$), while the dark lithology shows 4.65 ± 0.09 ($n = 39$) (where χ_0 is in 10^{-9} m^3 kg^{-1}). Thus, Chelyabinsk is three times more magnetic than the average LL5 fall, but is similar to a subgroup of metal-rich LL5 chondrites (Paragould, Aldsworth, Bawku, Richmond) and L/LL5 chondrites (Glanerbrug, Knyahinya). The meteorite's room-temperature magnetization is dominated by multidomain FeNi alloys taenite and kamacite (no tetrataenite is present). However, below approximately 75 K remanence is dominated by chromite. The metal contents of the light and dark lithologies are 3.7 and 4.1 wt%, respectively, and are based on values of saturation magnetization.

INTRODUCTION

On February 15, 2013 a small asteroidal fragment exploded at 9:22 am local time (03:22 UT) in a spectacular atmospheric fireball in the Chelyabinsk region of Russia. It was recovered in the form of the Chelyabinsk meteorite shower (LL5, S4, W0) immediately and shortly after the fall. Different aspects of the Chelyabinsk airburst event, including the reconstruction of the Chelyabinsk meteoroid orbit (Borovicka et al. 2013), damage assessment (Popova et al. 2013), mass and size distribution of the

Chelyabinsk meteorite fragments (Badyukov and Dudorov 2013), petrology, and geochemistry (Galimov et al. 2013) and others have already been investigated, whereas a thorough magnetic characterization of the Chelyabinsk meteorite remains lacking.

The magnetic properties of meteorites are effective tools for meteorite classification (Rochette et al. 2003, 2008, 2009b) and can contribute to our understanding of the physical conditions within the early solar system and the magnetic fields therein (e.g., Weiss et al. 2010).

The existing database of meteoritic low-field magnetic susceptibility χ_0 includes thousands of meteorites: ordinary chondrites (Rochette et al. 2003), nonordinary chondrites (Rochette et al. 2008), and achondrites (Rochette et al. 2009b). This database has been a valuable tool for the rapid classification of meteorites (e.g., Kohout et al. 2010), as well as the detection of misclassified and misidentified samples (Rochette et al. 2009a). The magnetic classification of meteorites is easy to apply and informative because χ_0 measurements are fast (few seconds per measurement) and nondestructive (see below), and can be conducted either in the laboratory or in the field. It is particularly useful for the classification of ordinary chondrite falls because the three classes (H, L, and LL) show nonoverlapping ranges of χ_0 (Rochette et al. 2003).

Raw values and preliminary magnetic measurements on a subset of the Chelyabinsk meteorite were previously published as a data brief (Bezaeva et al. 2013) in the Russian journal *Geochemistry International*. The purpose of this study was to present a more comprehensive characterization of the meteorite's magnetic mineral assemblage based on a larger number of samples and a broader range of experimental techniques, and to more fully develop our interpretation of the remanence preserved within the meteorite as well as to clarify the nature of clear outliers found in the Chelyabinsk collection (i.e., the samples with $\log\chi_0$ values from H chondrites' range). Measurements were conducted on the collection of Chelyabinsk fragments of Russian Academy of Sciences (RAS) maintained by the Vernadsky Institute of Geochemistry and Analytical Chemistry RAS (further referred to as Vernadsky Institute), and include low-field magnetic susceptibility, the anisotropy of magnetic susceptibility (AMS), hysteresis loops, back-field remanence demagnetization curves, first-order reversal curves (FORC), low-temperature magnetometry (10–300 K), thermomagnetic measurements (300–1073 K), Mössbauer spectroscopy, microprobe analyses, and X-ray microtomography. This thorough characterization effort aims to provide researchers with additional information about the origin of the Chelyabinsk meteorite and whether it is capable of retaining information about the magnetic environment of the early solar system.

SAMPLES AND MEASURING TECHNIQUES

Description of Samples

The Chelyabinsk airburst event resulted in thousands of stones that fell as a shower to the south and southwest of the city of Chelyabinsk, Russia. The first scientific expedition by the Vernadsky Institute to the Chelyabinsk region examined the area close to Deputatsky, Pervomaysky, and Emanjelinka villages immediately or within 2 weeks of the fall and resulted in the collection of 464 meteorite fragments with a total mass approximately 3.5 kg. All of the fragments were entirely or partially covered by fusion crust with a typical thickness ≤1 mm.

Polished surfaces of the stones showed them as consisting of two intermixed lithologies, with the majority (approximately 67%) being a light-colored lithology or variety (further referred to as LV) with a typical chondritic texture. This LV material was classified as a LL5 chondrite based on textural observations and mineral chemistries (Galimov et al. 2013). Bulk and grain densities (ρ_b and ρ_g, respectively) of LL ordinary chondrites (number of samples $n = 12$, falls only) are $\rho_b = (3.28 \pm 0.10)$ g cm^{-3} and $\rho_g = (3.55 \pm 0.04)$ g cm^{-3}, respectively (Consolmagno et al. 2006). Kohout et al. (2014) report the following bulk and grain densities for the LV and the DV of the Chelyabinsk chondrite: $\rho_b = (3.32 \pm 0.09)$ g cm^{-3} (LV, $n = 18$) and $\rho_g = (3.51 \pm 0.07)$ g cm^{-3} (LV, $n = 14$); $\rho_b = (3.27 \pm 0.08)$ g cm^{-3} (DV, $n = 7$) and $\rho_g = (3.42 \pm 0.10)$ g cm^{-3} (DV, $n = 7$).

The fifth petrological type refers to the degree of thermal metamorphism, and is based on a peak metamorphic temperature for the Chelyabinsk material of approximately 680 °C, derived using the olivine-chromite geothermometer. Chondrules in the LV mostly show angular boundaries and are easily delineated within a fine-grained fragmental matrix. The main minerals are olivine, orthopyroxene, and feldspar, with minor concentrations of high-Ca pyroxene and low-Ca clinopyroxene grains. Opaque phases include troilite (4 vol%), metallic FeNi (1.3 vol%) in the form of kamacite (body-centered cubic α-phase with Ni ≤7%) and taenite (face-centered cubic γ-phase with Ni ≥7%), accessory chromite (see below), and ilmenite. Olivine grains display mosaicism and parallel arrays of planar fractures—usually one or two sets per grain, but up to three sets per grain. Small plagioclase grains (<50 μm in size) rarely show planar deformation features. The shock effects in the LV correspond to S4 shock stage (Stöffler et al. 1991). Larger fragments of the LV are transected by thin (≤1 mm) black shock veins, which consist of a fine-grained shock melt containing clasts of

olivine and pyroxene with the same compositions as those in the LV.

The second lithology (approximately 33% by area) within the Chelyabinsk meteorite fragments is a dark variety (further referred to as DV). This material includes (1) blackened chondritic material with a chondritic texture and abundant, thin metal-sulfide veins; (2) impact melt breccia consisting of blackened chondrite fragments embedded in a fine-grained impact melt matrix, and (3) impact melts containing numerous metal-sulfide droplets and blebs, and rare mineral fragments. Indeed, most of the DV fragments appear to be ≤1.5 cm thick melt dikes and clasts of blackened chondrite. The blackening is caused by the presence of cracks and fractures that are infilled by extremely fine veins of metal-sulfide. The chondritic clasts also have thin, black-colored shock melt veins (approximately 0.05 vol%, a typical thickness is ≤1 mm), which most likely formed as a result of large impact event on the parent body after the LV and DV had already formed.

The melt dikes are composed of a cryptocrystalline matrix loaded with small (approximately 10 μm) euhedral olivine crystals, troilite–metal globules and inclusions, as well as clasts of olivines from the main chondritic mass, sometimes with recrystallization structures. The melt dikes can be formed either (1) in situ by melting of the chondrite due to shear stresses that were produced simultaneously with the thin shock veins or (2) by injection of impact melt into the weakened chondrite body. DV can also be designated as an impact melt breccia, taking into account the relatively large amount of impact melt matter in the dark lithology (approximately 30% and greater in existing sections).

The bulk compositions of the LV and DV lithologies are nearly identical (Galimov et al. 2013). Petrologic investigation of the collection revealed very few "mixed samples" consisting of both the light and the dark lithologies (Galimov et al. 2013).

The following minerals found in the Chelyabinsk meteorite may potentially be of interest for further magnetic interpretation: Fe-Ni alloys (kamacite, taenite), chromite (0.05 wt% with Mg and Al: Fe/[Fe+Mg] = 0.90, Cr/[Cr+Al] = 0.86 [atomic ratio]), and troilite (FeS). The mean composition of kamacite is 5.15 wt% Ni, 1.80 wt% Co, and 93.05 wt% Fe, while the mean composition of taenite is 35.3 wt% Ni, 0.86 wt% Co, and 63.84 wt% Fe. The chemistry of Chelyabinsk chromite is typical for LL chondrites (Wlotzka 2005). Other details on petrography and mineralogy of the Chelyabinsk meteorite can be found in Galimov et al. (2013). Preliminary mineralogical studies indicate that taenite/kamacite ratio in the metallic phase of the Chelyabinsk chondrite is approximately 4 (e.g., 20 wt% kamacite versus 80 wt% taenite). Figure 1 displays a "typical" metallic grain.

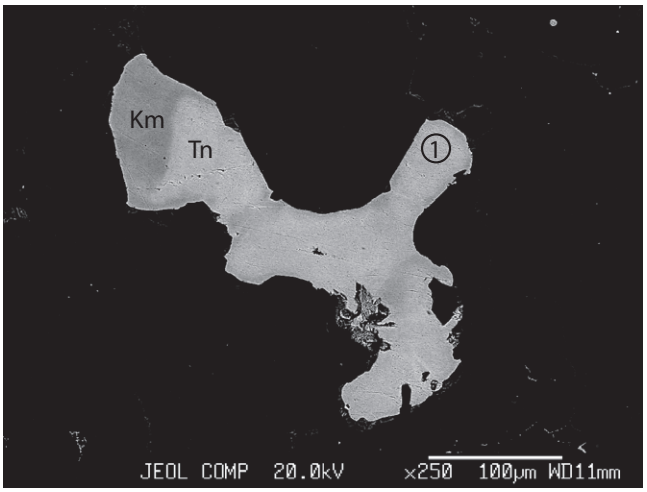

Fig. 1. Electron microprobe backscatter image of a "typical" metallic grain in the Chelyabinsk meteorite (sample 10–90, DV); "*Km*" indicates kamacite and "*Tn*" indicates taenite. Microprobe data presented in Table 5 (first column from the left) were collected from the point No 1 (indicated on the image).

Figure 2 shows backscattered electron micrographs for the LV (Fig. 2a) and the DV (Fig. 2b). Scanning electron microscopy reveals that metallic grains occur in a variety of sizes, ranging from micrometers to millimeters in the LV and up to >200 μm in the DV. On average, metallic grains are smaller in the DV. Interestingly, metallic grains in chondritic clast fragments in both the LV and the DV have similar grain size distributions, whereas the metallic grains in the impact melt matrix of the DV are noticeably smaller (10–50 μm). Apart from these fine metallic grains, the DV also contains vein networks of fine metallic material (Fig. 2b, lower middle; the network of very fine veins in the upper portion of the same figure consists of sulfides).

Rochette et al. (2003) demonstrated that the fusion crust's contribution to low-field magnetic susceptibility (χ_0) is negligible for samples with masses ≥3 g (approximately 1 cm^3), due to its exceedingly small surface area-to-volume ratio. Hence, we measured χ_0 for 174 fresh fragments (135 LV and 39 DV) weighing >3 g to determine the χ_0 distribution in the collection of Chelyabinsk meteorite fragments in Moscow. These fragments represent >80% of all samples with masses >3 g. Each sample was measured three times in mutually perpendicular directions to average the effects of anisotropy. Table 1 reports mean χ_0 values for some subspecimens. Most initial fragments were fully covered by fusion crust generated during the airburst.

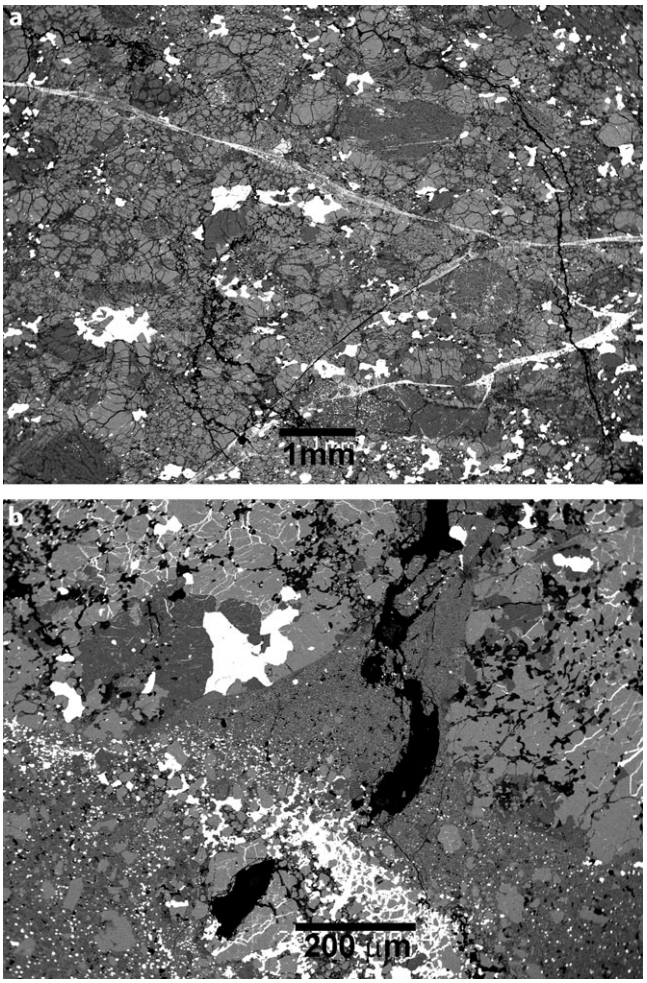

Fig. 2. SEM backscattered electron micrographs of the Chelyabinsk chondrite. a) The light lithology with a typical LL5 chondrite texture. Partly recrystallized chondrules have angular and rounded outlines. Shock veins (light gray strips) transect the meteorite mass. Sulfide and metal are white, olivine is light gray, low-Ca pyroxene is medium gray, and plagioclase is dark gray. b) The dark lithology consists of blackened chondrite clasts (upper right and left) cemented by a melt dike (lower left). Black patches are not related to the natural porosity of the material: they were formed by chipping of epoxy resin during preparation of the corresponding thin section and are exclusively due to the polishing procedure.

Two samples fully covered by fusion crust were used for more detailed magnetic measurements (see below): sample 11–12 (10.4 g) consists entirely of LV, while sample 10–126 (7.8 g) consists solely of DV. Both samples were cut into smaller subspecimens using a water-cooled low-speed saw, after which the fusion crust was removed using a Dremel drill with special nonmagnetic circular head (the fusion crust was not removed on a few subsamples for comparison). These subspecimens were removed from the central portions of meteorite fragments and shaped into cubic samples whenever possible. Sample masses are presented in Table 1.

Mössbauer spectra were acquired at room temperature for one LV sample, one DV sample, and one mixed sample. All three spectra are very similar and are composed of one doublet and one sextet, each reflecting paramagnetic iron Fe^{2+} and metallic Fe-Ni, respectively. The LV sample is much richer in paramagnetic iron when compared with the DV and mixed samples, which are similar to one another. Mössbauer spectra acquired at 77 K were noisy and thus not informative. Oshtrakh et al. (2013) acquired Mössbauer spectra with high-velocity resolution at 295 K on a LV sample and found six components in the Chelyabinsk chondrite: metal phase (1.7%), troilite, olivines (two components), and pyroxenes (two components). These results are in agreement with previously published studies of ordinary chondrites by Mössbauer spectroscopy with high-velocity resolution (Oshtrakh et al. 2008).

Instruments and Methods

Low-field susceptibility and AMS measurements were collected at the Vernadsky Institute using a IMVO-M susceptometer by Geologorazvedka, which measures χ_0 in the 10^{-7} to 10^{-1} SI range (assuming a nominal sample volume of 100 cm^3) using an alternating magnetic field amplitude of 300 A/m and a frequency of 1.025 kHz, and a relative error of ≤6.2%. AMS was quantified for select samples using the 15-position protocol of Jelinek (1978). Table 2 shows two scalar parameters characterizing AMS: the shape parameter T and degree of anisotropy ratio P. Field amplitude and frequency dependence of χ_0 were measured at CEREGE (Aix-en-Provence, France) using a MFK1-CS3 AGICO apparatus with three different frequencies (f_1 = 976 Hz, f_2 = 3904 Hz, f_3 = 15616 Hz) and alternating magnetic field amplitudes in the 5–700 A/m range.

For all of the remaining experiments described below, subspecimens of 11–12 (LV) and 10–126 (DV) were used. For those subsamples χ_0, AMS, and $\chi_0(T)$ up to 700 °C (heating–cooling cycle under argon atmosphere) were measured at the Institute for Rock Magnetism (IRM) at the University of Minnesota in Minneapolis, USA. χ_0 and AMS were measured using a KLY-2 AGICO apparatus (300 A/m, 920 Hz, and a nominal sensitivity of 4×10^{-8} SI, assuming a nominal sample volume of 10 cm^3). The natural remanent magnetization (NRM) and saturation isothermal remanent magnetization (SIRM), as well as their corresponding alternating field (AF) demagnetization spectra, were measured using a 2G Enterprises Model

Table 1. Main rock magnetic properties of the light variety (LV) and the dark variety (DV) of the Chelyabinsk meteorite.

Sample ID	m	χ_0	χ_{hf}	NRM	SIRM	MDF_i	M_s	M_{rs}/M_s	B_c	B_{cr}	B_{cr}/B_c
LV (no fusion crust)											
l-1	176	29.7	506	4.5	1312	7	6.3	0.002	0.5	24	48.0
l-2	177	41.6	–	11.6	2072	10	–	–	–	–	–
l-3	154	28.3	–	12.6	1511	6	–	–	–	–	–
l-4	101	27.8	–	7.0	1256	8	–	–	–	–	–
l-5	250	21.5	311	4.8	1113	8	4.8	0.003	0.6	19	31.7
l-6	298	29.7	189	9.2	1386	7	6.8	0.002	0.6	20	33.3
l-7	130	25.4	416	10.3	1213	7	5.2	0.003	0.6	32	53.3
l-8	222	41.5	–	27.8	3354	8	–	–	–	–	–
l-9	99	32.7	311	6.9	1880	7	7.4	0.003	0.6	19	31.7
Mean	179	30.9	347	10.5	1677	8	6.1	0.003	0.6	23	39.6
LV (with fusion crust)											
l-01	114	23.1	–	26.9	3970	–	–	–	–	–	–
l-02	156	31.1	482	38.5	4159	14	6.0	0.008	1.6	25	15.6
l-03	55	38.1	229	141.3	11561	14	8.7	0.009	2.4	28	11.7
Mean	108	30.8	356	68.9	6563	14	7.4	0.009	2.0	27	13.7
DV (no fusion crust)											
d-1	337	34.2	–	9.0	5339	5	–	–	–	–	–
d-2	405	31.8	459	7.9	5108	6	6.5	0.007	1.7	19	11.2
d-3	391	34.0	249	52.2	5514	5	7.1	0.008	1.7	12	7.1
d-4	390	33.1	–	10.1	5078	5	–	–	–	–	–
d-5	242	31.6	–	56.3	4382	6	–	–	–	–	–
Mean	353	32.9	354	27.1	5084	5	6.8	0.008	1.7	16	9.2
DV (with fusion crust)											
d-01	181	25.9	–	11.5	4792	10	–	–	–	–	–
d-02	119	41.5	1193	46.1	6133	6	7.2	0.009	1.7	16	9.4
d-03	102	33.9	254	17.7	5686	7	7.5	0.008	1.8	17	9.4
d-04	96	29.3	194	53.0	6425	6	6.5	0.008	2.1	18	8.6
Mean	125	32.7	547	32.1	5759	7	7.1	0.008	1.9	17	9.1

m is mass (in mg), χ_0 is low-field magnetic susceptibility (in 10^{-6} m^3 kg^{-1}), χ_{hf} is high-field magnetic susceptibility (in 10^{-9} m^3 kg^{-1}), NRM is natural remanent magnetization (in 10^{-5} Am^2 kg^{-1}), SIRM is isothermal remanent magnetization (in 10^{-5} Am^2 kg^{-1}), MDF_i is median destructive field of SIRM (in mT), M_s is saturation magnetization (in Am^2 kg^{-1}), M_{rs} is saturation remanent magnetization, B_c is coercivity (in mT), B_{cr} is coercivity of remanence (in mT).

760 SQUID (superconducting quantum interference device) cryogenic magnetometer, equipped with an inline AF demagnetizer. This magnetometer allows for the measurement of moments up to 10^{-4} Am^2 with a practical background noise level of 10^{-11} Am^2 and AF demagnetization up to fields of 170 mT. A 1T SIRM was imparted using a 2G Enterprises 670 pulse magnetizer. Low-temperature (10–300 K) magnetic measurements included FC-ZFC (field-cooled—zero-field-cooled) remanence and RT-SIRM (room-temperature SIRM) cooling-heating cycles, and were collected using a Quantum Design's MPMS2 (magnetic property measurement system 2), allowing the measurement of magnetic moment in the 10^{-10} to 10^{-3} Am^2 range under applied magnetic fields ranging from 0 to 5 T. The MPMS was also used to measure the frequency dependence of χ_0 in the 10–300 K range ($F_1 = 1$, $F_2 = 10$, and $F_3 = 100$ Hz frequencies were used). Major hysteresis loops (with parameters such as saturation magnetization M_s, saturation remanent magnetization M_{rs}, coercivity B_c), back-field demagnetization remanence curves (with main parameters such as M_{rs} and coercivity of remanence B_{cr}), and FORCs were measured at temperatures ranging from 10 K to 973 K using a Princeton Micromag vibrating sample magnetometer (VSM). FORC data were processed into FORC diagrams using the VARIFORC protocol of Egli (2013) within the FORCinel software of Harrison and Feinberg (2008). All FORC data were processed with the following VARIFORC parameters: Sc0 = 3, Sc1 = 7, Sb0 = 7, Sb1 = 7, and λv, h = 0.1. The same VSM was also used to collect thermomagnetic measurements, which monitor the saturation magnetization (M_s) in a 1T field as a function of temperature up to 973 K (700 °C) in a constantly flowing stream of heated helium gas to inhibit oxidation. Thermomagnetic curves up to 800 °C (two consecutive heating–cooling cycles) were measured

Table 2. AMS results for the Chelyabinsk chondrite samples.

Sample ID	m	$\log\chi_0$	P	T
Light variety				
4–91	3.82	4.58	1.392	0.626
10–4	4.69	4.77	1.288	0.650
11–19	5.50	4.58	1.343	0.606
11–18	7.20	4.52	1.233	0.227
7–8	4.78	4.39	1.233	0.572
10–123	3.50	4.44	1.063	0.632
Mean	–	4.55	1.259	0.552
Dark variety				
10–36	5.82	4.83	1.197	0.024
10–20	10.64	4.65	1.281	0.544
10–16	4.83	4.65	1.224	0.539
4–72	5.49	4.76	1.221	0.174
10–95	5.90	4.68	1.258	0.915
10–126	7.80	4.56	1.197	0.264
10–136	5.60	4.71	1.319	0.610
Mean	–	4.69	1.242	0.439
Anomalous sample 11–33				
11–33	4.6	5.47	1.431	0.752

m is mass (in g); χ_0 is low-field magnetic susceptibility (in 10^{-9} m^3 kg^{-1}); P and T are the degree of anisotropy of magnetic susceptibility (AMS) and AMS shape parameter, respectively.

in open air using a custom-made thermo-VSM (of N.M. Anosov and Y.K. Vinogradov design) with maximum applied field of 1T, with a nominal sensitivity of 10^{-8} Am^2. Mössbauer spectra were acquired at room T and 77 K using a Ranger Scientific Mössbauer Spectrometer at the IRM.

Thermal demagnetization spectra of NRM and SIRM (demagnetized using a 4 mT AF treatment prior to heating experiments to erase viscous magnetization components) were measured for two LV samples (*l-a* and *l-b*) and two DV samples (*d-a* and *d-b*) using MMTD80 furnace by Magnetic Measurements Ltd., where the magnetic field inside the furnace was reduced to <3 nT) and a 2G Enterprises SQUID magnetometer at CEREGE. All heating experiments were carried out under argon atmosphere using the following temperature sequence: 25, 120, 160, 200, 250, 300, 350, 400, 450, 500, 550, and 600 °C (with one-hour heating at each temperature step and corresponding postheating measurements).

Scanning electron microscopy (SEM) studies of polished meteorite samples were accomplished using a Zeiss ULTRA plus FESEM at the Center of Microscopy and Nanotechnology, University of Oulu (Finland), and a JEOL JSM-6480LV ASEM at the Institute of Petrology, M.V. Lomonosov Moscow State University.

Three-dimensional images of two DV samples (see below) were acquired by an X-ray Microtomograph MicroXCT-400 at CEREGE under the following operating conditions: 10W power supply, 4.3 μm voxel size, 2 s-per-view exposition time, and approximately 4.5 mm exposition zone.

Electron microprobe analyses were carried out using a JEOL JXA-8200 WD/ED combined microanalyzer at the Institute of Geology of Ore Deposits, Petrography, Mineralogy and Geochemistry, Russian Academy of Science operated using a 20 kV accelerated voltage and a beam current of 20 nA with counting time of 10 sec for main elements and 20 sec for accessory elements (the electron beam diameter is approximately 1 μm). International standards were used to calibrate the microprobe measurements and were selected such that their compositions were as similar as possible to the investigated phases of the Chelyabinsk meteorite.

EXPERIMENTAL RESULTS

Magnetic Susceptibility and AMS of the Chelyabinsk Collection

The mean $\log\chi_0$ for the LV is 4.57 ± 0.09 (1σ, $n = 135$) with a maximum (minimum) value of 4.77 (4.27) (in this study, $\log\chi_0$ is always calculated where χ_0 is reported in units of 10^{-9} m^3 kg^{-1}). The mean $\log\chi_0$ for the DV is 4.65 ± 0.09 (1σ) ($n = 39$) with a maximum (minimum) value of 4.88 (4.43), excluding two outliers (see below). Thus, the DV appears to be richer in magnetic metal than the LV. Figure 3 displays mean $\log\chi_0$ versus petrographic grade for LL, L, LL/L, and H chondrites, as well as for both lithologies of the Chelyabinsk meteorite, based on an updated database with respect to Rochette et al. (2003). As shown in Fig. 3, the Chelyabinsk chondrite does not fall into the "standard" LL5 range. The susceptibility of Chelyabinsk (LV) is three times higher than that of the average LL5 fall, but is similar to a subgroup of other metal-rich LL5 (Paragould, Aldsworth, Bawku, Richmond), as well as L/LL5 chondrites (Glanerbrug, Knyahinya, Qidong). In particular, the average value for Paragould, 4.56 ± 0.07, is indistinguishable from the LV value. There is no dependence of $\log\chi_0$ on sample mass for either lithology, which agrees with the conclusion that $\log\chi_0$ values are mass independent for the samples with $m > 3$ g (Rochette et al. 2003). In the case of the LV material, $\log\chi_0$ dispersion increases with decreasing sample mass (especially below 30 g).

Only two clear outliers were found among the 174 studied samples. The first clear outlier, the sample 10–90 (3.7 g) with $\log\chi_0 = 5.24$, was first reported by Bezaeva et al. (2013), but its nature was not discussed. The second outlier is the sample 11–33 (4.6 g) with $\log\chi_0 = 5.47$. Both samples are samples of DV. Such

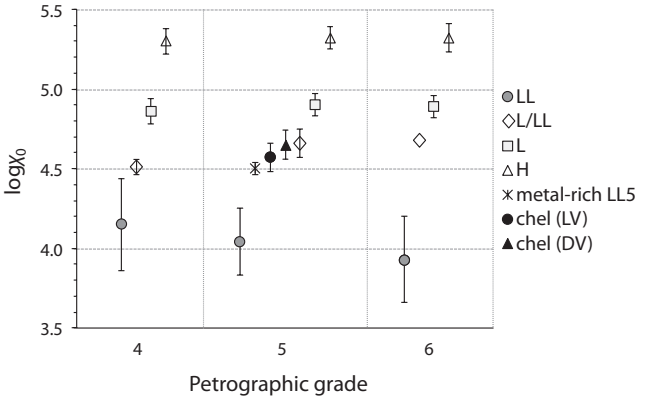

Fig. 3. Mean decimal logarithm of mass-specific magnetic susceptibility $\log\chi_0$ (in 10^{-9} m^3 kg^{-1}) with 1-sigma error bars versus petrographic grade for H (triangles), L (squares), L/LL (diamonds), and LL (circles) chondrites (falls only) from the updated database of Rochette et al. (2003). Additional filled points correspond to the light variety (LV) (circle) and the dark variety (DV) (triangle) of the Chelyabinsk meteorite. The asterisk shows a subgroup of other metal-rich LL5 chondrites (falls only: Paragould, Aldsworth, Bawku, Richmond). Petrographic grades are separated by vertical lines. Please note that points inside a single petrographic grade region all have the same petrographic grade, but are sorted by increasing $\log\chi_0$ and offset for added clarity.

high $\log\chi_0$ values are more typical for H chondrites. The unusual nature of these outliers is examined in more detail below (see discussion).

Histograms of $\log\chi_0$ distribution for both the LV and the DV are shown in Fig. 4. There are two peaks for the LV (where the left and right peaks will be further referred to as lower and upper peaks, respectively) and one broad peak for the DV (secondary peaks may reflect the brecciated nature of the DV, although the number of samples is not statistically high enough to robustly support such a statement). It is worth noting that the upper peak of the LV matches the main peak of the DV. This may indicate that some LV samples contain small fragments of DV material. Again, there is no correlation between the samples' masses and their $\log\chi_0$ values, as might be expected if this peak were due to larger samples containing fragments of DV material. So, although petrographic investigation of polished surfaces revealed very few mixed samples (Galimov et al. 2013), it is possible that such mixed samples are more prevalent. One potential explanation may be that the fusion crust on many of the meteorite fragments obscured the presence of DV material within fragments classified as LV. Indeed, mixed samples were also found in other Chelyabinsk collections (R. Jones, private communication). But as there is no clear idea of the fraction of mixed samples in the Chelyabinsk meteorite shower, we will further discuss only the LV and the DV.

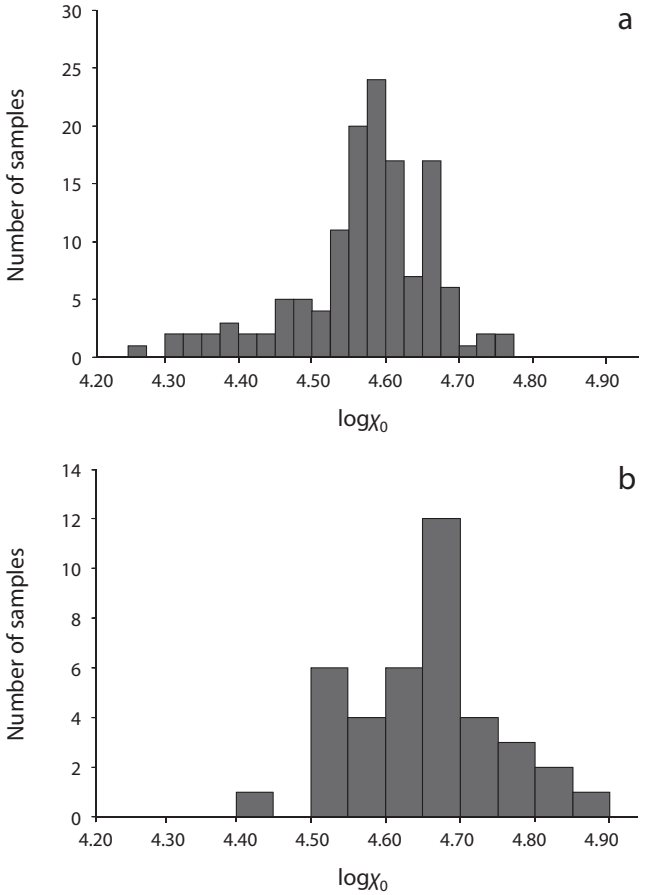

Fig. 4. Histograms of $\log\chi_0$ (in 10^{-9} m^3 kg^{-1}) for (a) the light variety and (b) the dark variety of the Chelyabinsk meteorite (two DV outliers are excluded, see text). Histogram interval is 0.025 for the LV and 0.05 for the DV.

Gattacceca et al. (2005) demonstrated that AMS can be used as an effective proxy for meteoritic petrofabrics and can be used as a marker of shock deformation in chondrites. Here, we report AMS data for 14 samples (6 LV samples and 7 DV samples and the anomalous sample 11–33) (Table 2). The degree of anisotropy (P) ranges from 6% to 39% with a mean value of 26% for the LV, and from 20% to 32% with a mean value of 24% for the DV. This is in good agreement with other published measurements on LL chondrites (Weaving 1962; Gattacceca et al. 2003, 2005). The general shape of the magnetic fabric in the Chelyabinsk meteorite is oblate (mean shape factor [T] is equal to 0.55 for the LV and 0.44 for the DV). The fact that the DV is as anisotropic as the LV suggests that the process responsible for anisotropy occurred after impact melting and affected the two lithologies equally. It is interesting to note that the anomalous sample 11–33 (DV) is much more anisotropic (P = 43%) than the average for the DV samples (P = 24%) (Table 2).

Measurements of the frequency dependence of susceptibility as a function of temperature (10–393 K) revealed little, if any, frequency dependence (<2.5%) for either the LV or DV material. Additionally, room-temperature measurements of the amplitude dependence of susceptibility (H) revealed little to no H dependence (<6%) for either the LV or DV material. However, room-temperature measurements of the frequency dependence of susceptibility at CEREGE (using f_1, f_2, f_3, see above) found values ranging from 6 to 16% for LV and 22 to 47% DV samples. We interpret this room-temperature frequency dependence as evidence for the presence of superparamagnetic (SP) grains (with typical grain sizes <23 nm; Kneller and Luborsky 1963) in the Chelyabinsk fragments.

Thermomagnetic Analyses

Thermomagnetic analyses are often used to identify the composition of constituent magnetic minerals via the determination of their Curie temperatures (T_c) (or diagnostic transition temperatures, e.g., $\alpha \rightarrow \gamma$). Here, we report results of the temperature dependence of low-field susceptibility, $\chi_0(T)$, as well as the temperature dependence of induced magnetization, $M_s(T)$.

$\chi_0(T)$ curves acquired for both the LV and the DV are presented in Figs. 5a and 5b, respectively. There is an indication of multiple Curie points on the heating curve in the 500–600 °C temperature range for the LV: both approximately 540 °C and approximately 590 °C Curie points are interpreted as an evidence for two families of taenite (Sugiura and Strangway 1988). Nonzero susceptibility at 700 °C (40% of overall room-temperature signal) indicates the presence of a phase with a T_c >700 °C, likely kamacite.

There is an evidence of multiple Curie points on the heating curve of DV in the 500–650 °C temperature range. T_c = 593 °C, determined using the inverse susceptibility method (Petrovsky and Kapicka 2006), most likely corresponds to taenite, whereas the higher T_c corresponds to kamacite. The remaining 12% χ_0 signal at 700 °C most likely reflects another family of kamacite grains.

Strong-field thermomagnetic curves $M_s(T)$, presented in Bezaeva et al. (2013), did not reach T_c of kamacite because of maximum attainable temperature being restricted to 700 °C. Here, we report additional measurements of $M_s(T)$ up to 800 °C for LV and DV (Figs. 6a and 6b, respectively). To assess the thermal stability of the meteorite, each sample was measured twice as it was heated from room temperature to 800 °C in open air at rate of 1 °C per second up to 600 °C followed by 0.33 °C per second above 600 °C. There are two characteristic points on the first heating curve for

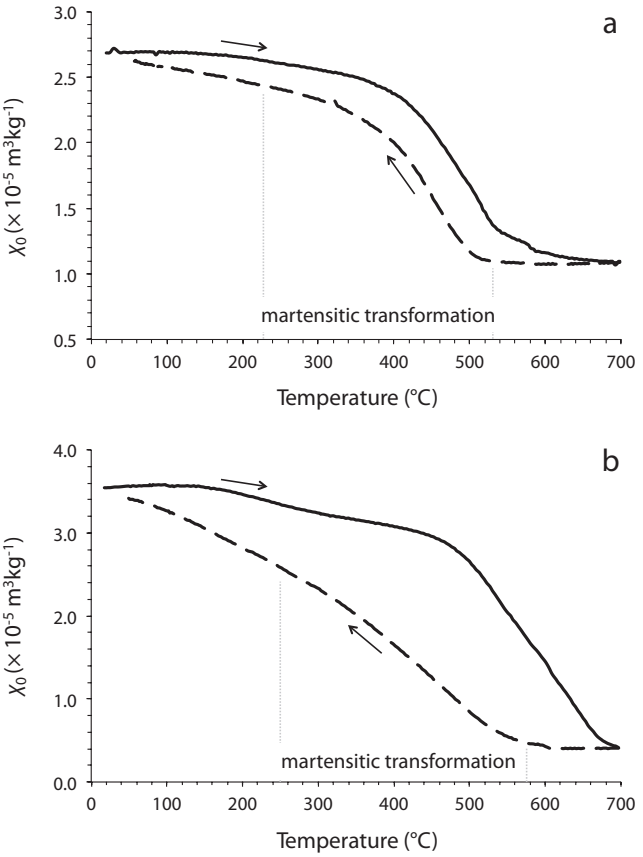

Fig. 5. Mass normalized, low-field magnetic susceptibility χ_0 versus temperature for (a) the light variety and (b) the dark variety of the Chelyabinsk meteorite. All curves were acquired under argon atmosphere. Solid lines correspond to heating cycles, whereas dashed lines correspond to cooling cycles (also indicated by the corresponding arrows). The temperature range of the martensitic transformation is indicated for each cooling curve.

the LV: approximately 500 °C and >760 °C, which reveal taenite and kamacite, respectively; whereas the two Curie points for the DV fall in the 650–770 °C temperature range and probably correspond to different populations of kamacite. It is important to note that bulk samples of LL chondrites, such as Chelyabinsk, are likely to contain a spectrum of FeNi phases with a wide grain size distribution and different Ni-content, which produces broad changes as samples are heated and cooled. The LV material shows largely reversible heating and cooling curves, suggesting that very little oxidation occurred during the experiment, while the DV showed only a moderate 18% drop in induced magnetization after two heating and cooling cycles. However, the main features of the induced magnetization remained constant for DV, and we do not observe any newly formed magnetite in either of the two heating curves or either of the two cooling curves. Thus, we conclude that oxidation is not a major

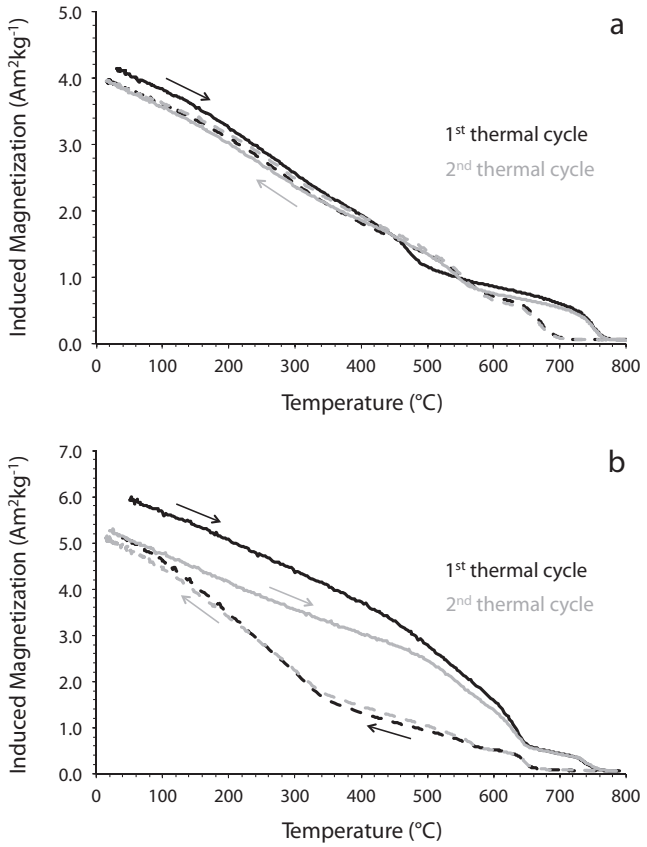

Fig. 6. Strong-field thermomagnetic curves for the (a) light lithology and (b) dark lithology of the Chelyabinsk meteorite. All curves were acquired in open air. Black lines correspond to the first heating-cooling cycle, whereas gray lines correspond to the second heating-cooling cycle. Solid lines indicate heating cycles and dashed lines indicate cooling cycles (also indicated by the corresponding arrows).

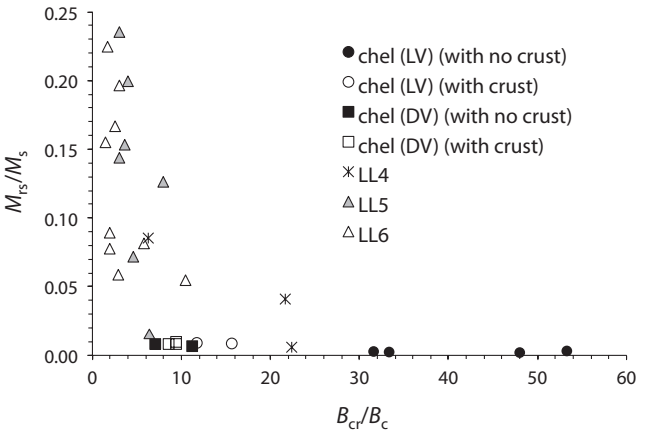

Fig. 7. Day plot showing M_{rs}/M_s versus B_{cr}/B_c for the light variety (LV) and the dark variety (DV) of the Chelyabinsk meteorite. Samples with and without fusion crusts are shown separately. Data for the other LL ordinary chondrites—LL4 (Benares, Savtschenskoe, Soko-Banja), LL5 (Alta'ameem, Guidder, Konevo, Nyirabrany, Olivenza, Siena, Tuxtuac), and LL6 (Appley Bridge, Benguerir, Bensour, Douar Mghila, Dhurmsala, Jelica, Kilabo, Manbhoom, Oued el Hadjar, Saint-Severin, Vavilovka)—come from Gattacceca et al. (2014). M_s and M_{rs} are saturation magnetization and saturation remanent magnetization, while B_c and B_{cr} are coercivity and coercivity of remanence, respectively. Chelyabinsk samples are highly multidomain and are different from most other LL5 chondrites, in that they show lower remanence ratios. In contrast to the Chelyabinsk meteorite, most of other LL5 chondrites contain tetrataenite, and thus are characterized by much higher B_c and B_{cr} values.

concern during these measurements. The cooling curves for both $\chi_0(T)$ and $M_s(T)$ show a martensitic transformation of fcc to bcc FeNi alloys. The susceptibility and thermomagnetic curves for the LV are more reversible and show lower thermal coercivities than those of the dark material. It is likely that the DV is more enriched in kamacite than the LV as a result of shock metamorphism processes.

No evidence was observed for the presence of tetrataenite in either lithology of the Chelyabinsk chondrite, as would be indicated by the presence of a characteristic transition temperature of approximately 550 °C on the heating curves (Wasilewski 1982, 1988).

Magnetic Hysteresis and Low-Temperature Magnetic Properties

Parameters derived from hysteresis measurements, such as the remanence ratio (M_{rs}/M_s) and the coercivity ratio (B_{cr}/B_c), can be used to interpret samples' average magnetic grain size, using a "Day Plot" (Day et al. 1977) or its modification after Dunlop (2002). Bezaeva et al. (2013) previously reported the results of room-temperature hysteresis measurements for the Chelyabinsk samples (Table 1). Figure 7 displays these data along with data from other LL chondrites (LL4, LL5, and LL6) for comparison. Typical (slope-corrected) hysteresis loops acquired in the 10–300 K temperature range are presented in Fig. 8 (see box). As stated earlier in Bezaeva et al. (2013) and as follows from Fig. 7 and Fig. 8 (box), the Chelyabinsk samples are magnetically soft (mean bulk coercivity, B_c<2 mT and mean coercivity of remanence, B_{cr} = 23 mT and 16 mT for the LV and the DV, respectively). Such low B_c and B_{cr} values provide further support for the absence of tetrataenite (e.g., Bezaeva et al. 2010). Indeed, tetrataenite-rich LL chondrites show mean $B_c = 40.7 \pm 31.5$ mT (n = 52) (Gattacceca et al. 2008) and $B_{cr} = 136.3 \pm 92.9$ mT (n = 28) (Gattacceca et al. 2014). Metallic grains from both lithologies are primarily multidomain (Figs. 7 and 8 box).

Figure 8 displays temperature dependence of B_{cr} for the light variety of the Chelyabinsk meteorite (sample *l-7*): upon cooling from room temperature down to

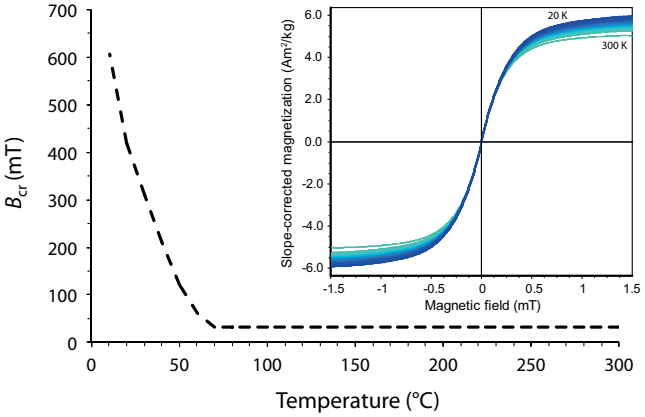

Fig. 8. Remanent coercivity B_{cr} versus temperature for the light variety of the Chelyabinsk meteorite (sample *l-7*). The dramatic decrease that plateaus at 32–33 mT at approximately 70 K corresponds to the Curie temperature of chromite. "In-box" figure: slope-corrected hysteresis loops for the same sample (*l-7*) of the Chelyabinsk meteorite acquired in the 20–300 K temperature range (the upper loop was acquired at 20 K and the lower loop was acquired at 300 K).

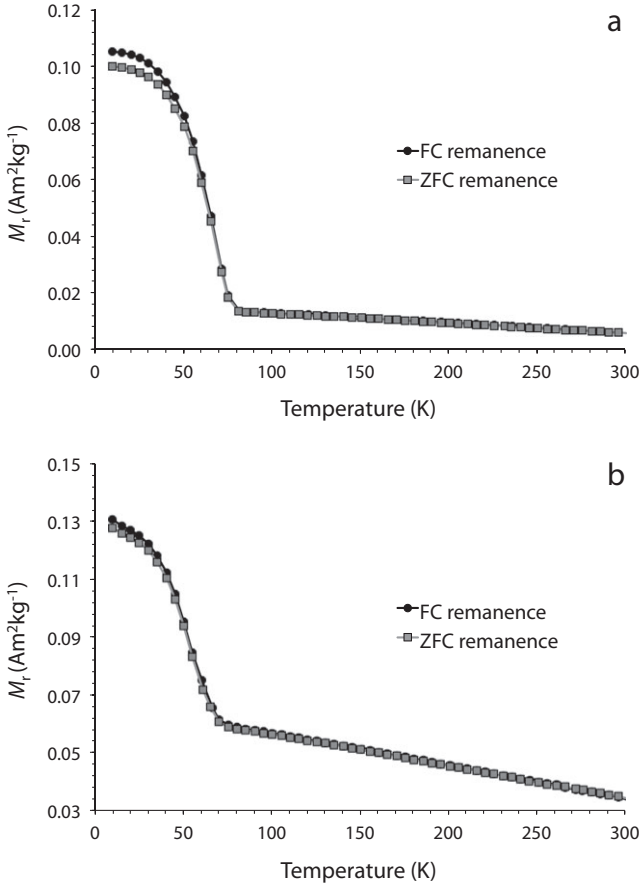

Fig. 9. FC (field-cooled)—ZFC (zero-field-cooled) remanence data set for (a) the light variety (sample *l-1*) and (b) the dark variety (sample *d-2*) of the Chelyabinsk meteorite. Crosses show a zero-field warming of a remanence acquired by field cooling from 300 K in a 2.5 *T* magnetic field; circles show zero-field warming of a remanence acquired isothermally in a 2.5 *T* at 20 K after zero-field cooling from 300 K. Nonlinearity below approximately 70–80 K corresponds to chromite present in the Chelyabinsk meteorite.

10 K, the Chelyabinsk meteorite is transformed stepwise from a magnetically soft material at room temperature to a magnetically hard material below approximately 70 K with B_{cr} = 606 mT for the LV at 10 K. The DV material produces a B_{cr} = 157 mT at 10 K. This magnetically hard phase is also detectable in the FC-ZFC remanence data set, presented in Fig. 9. There is a dramatic decrease in remanence for both lithologies of the Chelyabinsk meteorite in the temperature range 10 to 70–80 K (approximately 80 K for the LV and approximately 70 K for the DV) and only negligible monotonic changes above approximately 75 K. No evidence of the Verwey transition (approximately 110–120 K) is observed, providing further confirmation for the absence of magnetite in the Chelyabinsk samples, which is consistent with the typical mineralogy of ordinary chondrites.

First-order reversal curve (FORC) distributions (Fig. 10) provide information about the distribution of microscopic coercivities within a sample and the magnetic interactions between domains within magnetic mineral assemblages. Room-temperature FORC diagrams of the LV (Fig. 10a) and the DV (Fig. 10b) share many similarities, with both materials being dominated by low-coercivity grains with strong positive and negative interactions consistent with multidomain magnetic material. Marginal coercivity distributions from the room-temperature FORC diagrams show that the majority of grains within the LV have microscopic coercivities <10 mT (Fig. 10c), whereas the DV contains a slightly higher concentration of grains with coercivities >10 mT (Fig. 10d). These subtle differences may be an indication of the mean grain sizes within the two materials, where the DV cooled at a faster rate, and thereby contains a higher fraction of smaller grains. The absence of tetrataenite is confirmed by these FORC diagrams that are noticeably different from those obtained on tetrataenite-rich samples (Acton et al. 2007; Gattacceca et al. 2014).

The FORC distribution at 10 K for a sample of the light-colored lithology is shown in Fig. 10e. As in the room-temperature FORCs, most of the magnetic mineral assemblage is consistent with multidomain magnetic behavior. However, this low-temperature FORC also shows evidence of a very high coercivity phase whose microscopic coercivities range from 200 mT to 1100 mT and is offset below the Bu = 0 line. This high coercivity phase was not present in the room-temperature FORCs, yet its presence provides

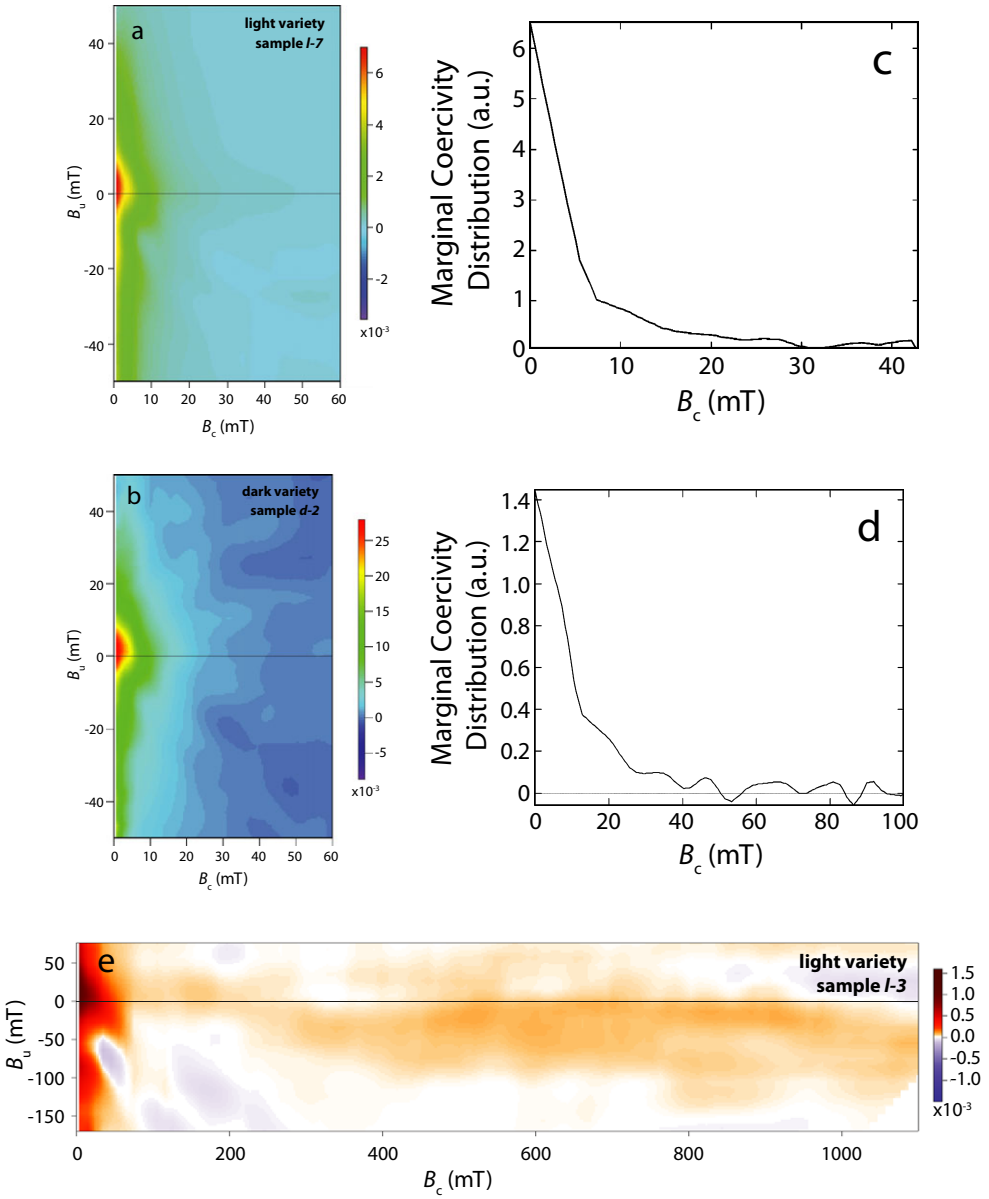

Fig. 10. FORC (first-order reversal curve) diagrams for (a) the light variety (LV) (sample *l-7*) and (b) the dark variety (DV) (sample *d-2*) of the Chelyabinsk meteorite collected at room temperature. Most of the coercivity distribution remains near the origin and is consistent with a population of multidomain grains, but the dark material displays a high range of coercivities in the marginal coercivity distribution. (c) Distribution of microcoercivities for the LV (sample *l-7*) and (d) the DV (sample *d-2*). e) FORC diagram for sample *l-3* (light variety) collected at 10 K. Most of the coercivity distribution remains near the origin, but a high coercivity phase is also present. This higher coercivity phase is likely chromite, displays coercivities ranging from 200 to 1100 mT, and is offset below the Bu = 0 line. All three FORC diagrams were processed using the VARIFORC protocol of Egli (2013) within FORCinel (Harrison and Feinberg 2008).

independent confirmation of the high coercivity phase that was seen in the B_{cr} and FC-ZFC data described above (Figs. 8 and 9).

Magnetic Remanence

The logM_{rs} for the LV (with no crust) falls within the range from 1.05 to 1.53 ($\times 10^{-3}$ Am^2 kg^{-1}) with a mean value of 1.20 ± 0.15. The logM_{rs} for the DV (samples with no crust) falls within 1.64 to 1.74 ($\times 10^{-3}$ Am^2 kg^{-1}) with a mean value of 1.71 ± 0.04 (in 10^{-3} Am^2 kg^{-1}). These values are roughly consistent with previously published data on LL5 and L/LL5 chondrites (Rochette et al. 2003): 1.45–2.89 ($\times 10^{-3}$ Am^2 kg^{-1}); but the mean value of logM_{rs} for the LV of the Chelyabinsk meteorite is lower than the

corresponding mean value from literature (although the $\log M_{rs}$ database is less complete than the corresponding $\log\chi_0$ database). Indeed, Gattacceca et al. (2014) report the following mean value for LL5 chondrites: $\log M_{rs} = 2.72 \pm 2.34$ ($\times 10^{-3}$ $Am^2\ kg^{-1}$) ($n = 7$). We interpret the distinctly lower values for the Chelyabinsk chondrite to be due to the absence of tetrataenite, which is present in most of the other LL chondrites in the $\log M_{rs}$ database.

AF demagnetization spectra of NRM and SIRM were acquired for all samples. As reported earlier in Bezaeva et al. (2013), the mean median destructive field (MDF_i) of SIRM is 8 mT for the LV and 5 mT for the DV (Table 1), which is consistent with low coercivity values of the Chelyabinsk meteorite at room temperature (see above).

Thermal demagnetization curves of NRM and SIRM for samples of LV and DV are presented in Fig. 11. Both materials show that their NRM is progressively demagnetized up to 400 °C, at which point only 19% and 7% of the remanence remains for the LV and DV, respectively. Both samples show irregular demagnetization behavior with increasing temperature above 400 °C due to unstable remanence. Thermal demagnetization of the SIRM also shows similarly low unblocking temperatures (Fig. 11b), and we observe that the SIRM of DV is more resistant to thermal demagnetization than that of LV.

To isolate stable components of magnetization and attempt to estimate the strength of the ancient field that originally magnetized the Chelyabinsk meteorite, we examined orthogonal projections (so-called Zijderveld plots or vector end-point diagrams) of NRM together with the ratios of equivalent magnetization (REM and REM′) paleointensity protocols of Gattacceca and Rochette (2004). The REM ratio is calculated as NRM/SIRM, and the corresponding paleofield is calculated in μT as REM × f, where f is a calibration factor (often with a value of 3000). The REM′ ratio is determined in a slightly different manner, where the slope of the NRM demagnetization curve at a given AF step (dNRM/dAF) is normalized by the slope of the SIRM demagnetization curve at the same AF step (dSIRM/dAF) giving $REM' = \Delta NRM/\Delta SIRM$. The corresponding paleofield in μT is calculated again as REM′ × f, where f is usually assumed to have a value of 3000. These isothermal paleointensity methods are frequently used in studies of meteorites, where materials are often highly sensitive to mineralogical alteration during heating. Lappe et al. (2013) recently showed that the calibration factors used in REM and REM′ paleointensity estimates may vary significantly for different materials, and thus the estimates reported here have a minimum uncertainty of about a factor of two.

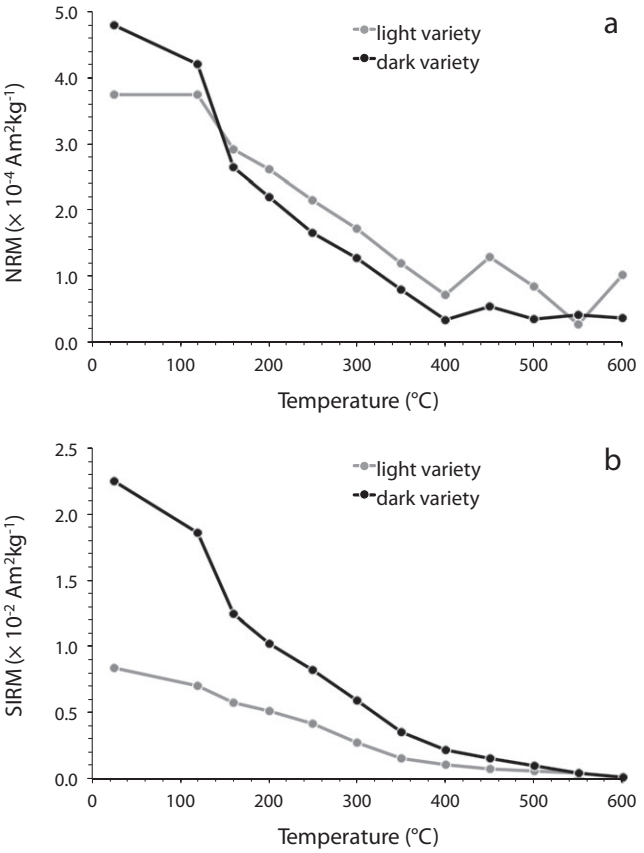

Fig. 11. Step-wise thermal demagnetization of (a) natural remanent magnetization (NRM) and (b) saturation isothermal remanent magnetization (SIRM) of the Chelyabinsk meteorite fragments up to 600 °C. All heating experiments were conducted under argon atmosphere in a reduced magnetic field (few nT) with 1 h thermal treatment per temperature step and remanence measurements in between heating steps. Gray line corresponds to the light variety and black line corresponds to the dark variety of the Chelyabinsk chondrite. Both samples were given an alternating field treatment of 4 mT prior to thermal demagnetization to remove viscous magnetization.

Unfortunately, most Chelyabinsk samples display demagnetization spectra that are too noisy to confidently define any stable components of magnetization. REM estimates for all samples (without fusion crust) are presented in Table 3. These paleofield values are likely to be overestimates, as the REM method tends to yield marginally higher paleointensities for metal-bearing meteorites enriched in multidomain material (with MDF_i<20 mT, as is the case for our samples, see Table 1) (Gattacceca and Rochette 2004). Two DV samples without fusion crust produced orthogonal projections with stable components of magnetization, they are discussed below. The first DV sample (*d-b*) displays REM′≈2% (up to AF = 30 mT) and thus, a paleofield approximately 50–60 μT. The second DV sample displays a paleofield approximately

Table 3. Estimated magnetic paleointensities (from REM method) of the Chelyabinsk samples.

Sample ID	Total REM (×1000)	$REM_{4\ mT}$ (×1000)	$REM_{10\ mT}$ (×1000)	Paleofield (μT)
LV (no fusion crust)				
l-1	3.41	2.44	3.56	10.2
l-2	5.62	3.68	4.36	16.9
l-3	8.37	8.86	10.46	25.1
l-4	5.58	3.77	8.86	16.8
l-5	4.34	3.68	6.46	13.0
l-6	6.64	6.71	7.25	19.9
l-7	8.52	5.93	5.91	25.5
l-8	8.29	4.41	5.99	24.9
l-9	3.66	2.40	9.68	11.0
Mean	6.28	4.50	6.70	18.8
DV (no fusion crust)				
d-1	1.69	0.93	1.27	5.1
d-2	1.56	0.89	2.13	4.7
d-3	9.47	1.32	1.81	28.4
d-4	2.00	1.64	1.55	6.0
d-5	12.84	5.08	4.06	38.5
Mean	5.33	1.88	2.14	16.0

REM = NRM/SIRM, where NRM is natural remanent magnetization and SIRM is saturation isothermal remanent magnetization. $REM_{4\ mT}$ and $REM_{10\ mT}$ are REM values after AF demagnetization up to 4 mT and 10 mT, correspondingly.

10 μT (estimated from REM′) for the low-coercivity component (below AF = 10 mT).

DISCUSSION

Metal Content of the Chelyabinsk Meteorite

The magnetic properties of the Chelyabinsk meteorite can be used to estimate its metal content. As stated earlier, from the point of view of χ_0, the Chelyabinsk meteorite does not fall into the "standard" LL5 range but shares many similarities with a subgroup of metal-rich LL5 and L/LL5 chondrites. χ_0 data allow an estimation of the meteorite's metal content using the calibration of Rochette et al. (2003): it was previously reported by Bezaeva et al. (2013) that the maximum χ_0-based metal content of the light-colored material is calculated as 6.9 wt%. Such a value is inconsistent with previously published modal mineral abundances, which reported metal contents <2 wt% (Galimov et al. 2013). The overestimation of the χ_0-based value for the metal content may be due to multiple factors, as low-field susceptibility can be influenced by many parameters other than mineral concentration including anisotropic metallic grains, magnetostatic interactions, inhomogeneous distribution of metallic grains, the presence of superparamagnetic grains, and the network of metallic veins (see Fig. 2b), all of which may artificially increase the measured value of χ_0.

An alternative method for estimating the metal content for the light and dark lithologies involves using the saturation magnetization values collected during hysteresis measurements and dividing them by known values of M_s for pure kamacite (220 $Am^2\ kg^{-1}$ [Sugiura and Strangway 1988]) and pure taenite (150 $Am^2\ kg^{-1}$ [Sugiura and Strangway 1988]). Using mean M_s values for LV and DV samples with no fusion crust (Table 1), and by taking into account that the metallic phase of our samples is composed of 20 wt% kamacite and 80 wt% taenite, we arrive at metal content estimates of 3.7 wt% and 4.1 wt% for LV and DV fragments, respectively (Bezaeva et al. 2013). These values represent a significant improvement over the χ_0-based estimate, owing to the fact that the M_s-based estimates are not affected by anisotropy, grain size, or spatial distribution of magnetic grains. Additionally, the M_s-based estimates are likely to be more accurate than the <2 wt% estimate of Galimov et al. (2013), which was derived by visual modal counting of SEM photomicrographs. Indeed, Galimov et al. (2013) themselves recognize that their value probably underestimates the true metallic content of the Chelyabinsk meteorite due to their inability to account for small metallic grains.

Figure 12 displays metal content as a function of $\log\chi_0$ for LL, L, L/LL, and H chondrites as well as the Chelyabinsk meteorite (both the LV and the DV). The metal content of both the LV and the DV of the Chelyabinsk chondrite are similar to both LL and L/LL chondrites. Indeed, Gattacceca et al. (2014) report the following metal contents for the LL chondrites (here and further only falls are considered): (2.94 ± 1.51) wt% (n = 14) and L/LL chondrites: (6.57 ± 1.16) wt% (n = 2) (these are revised results with regard to Jarosewich [1990] after reclassification of certain meteorites). Dunn et al. (2010) report the following metal content for LL5 chondrites: (3.8 ± 2.2) wt% (n = 5; the following LL5 chondrites were investigated: Aldsworth, Alta'ameem, Olivenza, Paragould, Tuxtuac). Given this context, we believe that the metal content of the Chelyabinsk chondrite is more similar to other LL chondrites, rather than the L/LL chondrites.

Variability of Low-Field Magnetic Susceptibility

The low-field magnetic susceptibility distribution of all investigated Chelyabinsk fragments (if we exclude two clear outliers, discussed below) is rather homogeneous: all scatter lies within a 3σ range for both the LV and the DV. The LV and DV differ from one another at the 2σ level. This allows us to conclude that

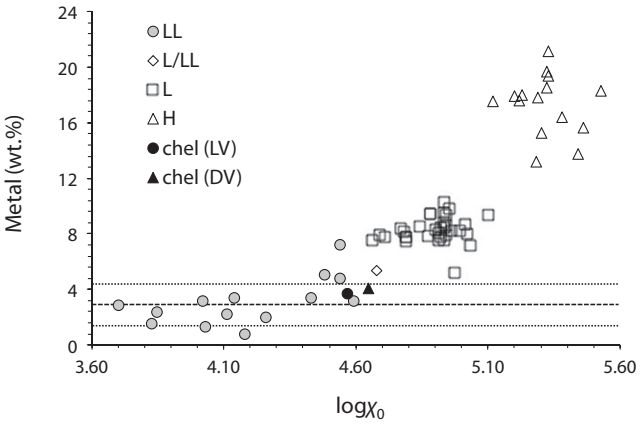

Fig. 12. Metal content (in wt%) versus $\log\chi_0$ for different groups of ordinary chondrites (LL, L/LL, L, H). $\log\chi_0$ data come from Rochette et al. (2003) and metal contents come from Jarosewich (1990) and Dunn et al. (2010) (for some LL chondrites). The light variety (LV) and the dark variety (DV) of the Chelyabinsk meteorite are indicated by the solid circle and the solid triangle, respectively. Dashed lines indicate mean metal content for LL chondrites (with s.d.): 2.94 ± 1.51 (Gattacceca et al. 2014). The only L/LL data point corresponds to the meteorite Knyahinya (L/LL5).

the Chelyabinsk parent body is relatively homogeneous on the scale of the investigated samples (several cm).

Additionally, the Chelyabinsk chondrite consistently shows the presence of superparamagnetic metallic grains, as confirmed by the strong room-temperature frequency dependence of χ_0. Moreover, the DV is richer in metallic iron nanoparticles than the LV. Van de Moortèle et al. (2007) previously reported superparamagnetic-sized, shock-induced metallic nanoparticles in olivine crystals from Martian meteorites. The DV of the Chelyabinsk meteorites may have been enriched in metallic nanoparticles by the same shock mechanism (especially in the black shock veins zones). However, no dark olivines were observed in the Chelyabinsk meteorites during petrological investigations, as were reported by Van de Moortèle et al. (2007).

The Absence of Tetrataenite

The absence of tetrataenite is one of the defining characteristics of the magnetic mineral assemblage of the Chelyabinsk chondrite. This absence is likely due to the shock and thermal history of the Chelyabinsk parent body. Gattacceca et al. (2014) conclude that in equilibrated chondrites (such as Chelyabinsk), shock-related heating above approximately 450–500 °C and its subsequent rapid cooling result in the disordering of tetrataenite into Ni-rich taenite. This transformation is accompanied by drastic changes in magnetic properties, such as a decrease in M_{rs}, B_c and B_{cr}—all of which are observed in the Chelyabinsk chondrite samples. This effect is maximal for S5 and S6 chondrites, but is already visible starting from shock stage S4 (see fig. 10 in Gattacceca et al. 2014), which displays M_{rs} and B_{cr} versus shock stage for L chondrites). Thus, these magnetic properties represent very sensitive proxies for the shock and thermal history of Chelyabinsk meteorite.

The Presence of Chromite

The presence of chromite in the Chelyabinsk chondrite was previously reported by Bezaeva et al. (2013); it produces dramatic low-temperature magnetic behavior. The observed Curie temperature of chromite in the Chelyabinsk meteorite (approximately 70–80 K) is consistent with previously published T_c for pure chromite (<80 K; Banerjee 1972). Chromite's T_c, its high coercivity, and its role as a remanence carrier are readily visible in the low temperature data presented above for both the LV and DV. This behavior is consistent with previously published data for ordinary chondrites (Gattacceca et al. 2011). Below 75 K, chromite dominates the magnetic remanence of the Chelyabinsk meteorite and is responsible for significant increase in B_c and B_{cr} values (Fig. 8). To isolate the magnetic hardness (B_{cr}) of chromite alone, we subtracted the back-field remanence demagnetization curve at 90 K from the corresponding curve at 20 K for both the LV and the DV samples (Fig. 13). Thus, B_{cr} of chromite at 20 K is 505 mT for the LV and 335 mT for the DV. The corresponding (uncorrected) values of 420 mT and 133 mT reflect a mixture of metal and chromite. This is in agreement with other ordinary chondrites containing chromite (discussed in Gattacceca et al. [2011]). For example (here and further: P. Rochette, unpublished data), the corrected values of B_{cr} at 20 K are 299 mT (Tuxtuac, LL5), 266 mT (Bensour, LL6), 305 mT (Siena, LL5), 450 mT (Savtschenskoe, LL4), 302 mT (Soko-Banja, LL4). These data are also consistent with the FORC distribution for LV at 10 K shown in Fig. 10e, which shows a high coercivity phase with microcoercivities ranging from approximately 200 mT to 1100 mT. Thus, the corrected B_{cr} (at 20 K) reflecting chromite of approximately 300 mT is typical for LL ordinary chondrites.

The Nature and Origin of Magnetically Anomalous Samples

Two of the 174 samples measured in this study revealed anomalously large susceptibility values. Both samples are composed of DV material: sample 11–33 (4.6 g) with $\log\chi_0 = 5.47$ (10^{-9} m^3 kg^{-1}), and sample 10–90 (3.7 g) with $\log\chi_0 = 5.24$ (10^{-9} m^3 kg^{-1}). The

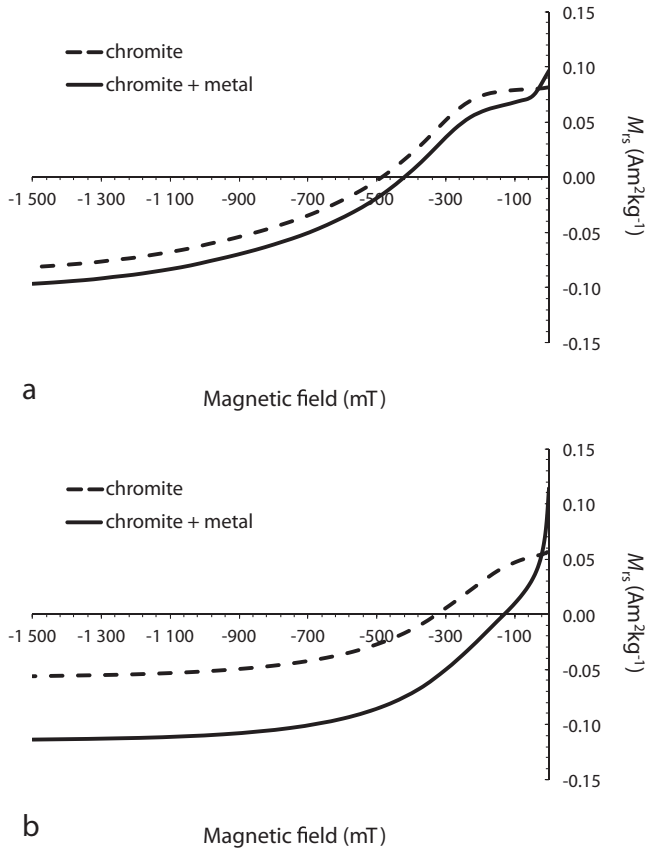

Fig. 13. Backfield remanence demagnetization curves (solid lines) acquired at 20 K for (a) a sample of the light variety and (b) a sample of the dark variety of the Chelyabinsk meteorite. Dashed lines correspond to pure chromite; they were obtained by subtraction from the presented curves of the corresponding backfield remanence curve, acquired at 90 K.

high logχ_0 value of the 11–33 is similar to that of H chondrites (see Fig. 3), and could be interpreted as an enclave of H-type chondrite within the Chelyabinsk meteorite shower. Such mixtures of different classes of chondrites have been noted in earlier studies. Indeed, a similar inclusion of H-type chondrite was found in the St. Mesmin LL6 chondrite (Chou et al. 1981). Furthermore, a centimeter-scale L-type clast has been described on the LL chondrite NWA 5764 (Gattacceca et al. 2009). Finally, Yanai and Kojima (1993) also reported a regolith breccia (Antarctic meteorite Yamato-8424) consisting of H and LL chondrite mixture. What follows below is a brief discussion of each sample that aims to determine whether or not these two samples may represent enclaves of a separate class of chondrite embedded within the Chelyabinsk meteorite shower.

Sample 11–33's susceptibility is seven times higher than that of the average DV sample and nine times higher than the metal-rich LL5 subgroup (Fig. 3). It also shows anomalously high magnetic anisotropy: its degree of anisotropy is 43% as compared to 24% for the average DV sample (Table 2). The sample has almost no fusion crust and visual inspection shows it to be enriched in sulfides. To clarify the nature of this sample, we imaged its internal structure using X-ray microtomography and compared it with similar imagery for a "standard" DV sample (10–126) (Fig. 14). Although it should be noted that this X-ray technique has a spatial resolution of 4 μm, and hence will not detect single domain (SD) and SP sized grains, it still allows us to make observations that are relevant to understanding the χ_0 and AMS data of the anomalous samples. The X-ray microtomography images show that the "standard" DV sample (10–126) contains a greater diversity of high-density magnetic minerals including Fe-sulfides and FeNi alloys. Generally, the largest metallic grains in 10–126 are smaller than the largest grains in 11–33. Furthermore, 10–126 contains interconnected veins of both sulfides and metals. By contrast, X-ray microtomography shows that the anomalous sample (11–33) contains only discrete grains of FeNi alloys. The anomalously high χ_0 observed in 11–33 is likely due to the presence of these large metallic grains. The diversity of magnetic materials in 10–126 produces a composite AMS signal, whereas the AMS in the anomalous sample is only influenced by the fabric of the FeNi alloys. Further work is required to investigate the distribution of aspect ratios of the grains in the anomalous sample to better understand the origin of its high degree of AMS. Regardless, it is likely that the sample 11–33 is simply a LL chondrite enriched in metal, and does not represent an enclave of a different chondrite class.

The other anomalous sample 10–90 was cut and a polished surface was prepared for further optical microscopy and electron microprobe analyses of olivines, orthopyroxenes, and metal (Tables 4 and 5). The approximate dimensions of the sample 10–90 are $2 \times 1 \times$ 1 cm. The sample is composed of typical ordinary chondrite minerals, including olivine, low-Ca pyroxene, plagioclase (maskelenyte), high-Ca pyroxene, troilite, metal, chromite, ilmenite, and traces of other accessory phases. The main mass of the sample consists of chondrules within a recrystallized matrix; outlines of the chondrules are generally poorly defined. Blackening of the main mass is caused by films of sulfides and metals that fill numerous irregular cracks and planar features in silicates and oxides. The main mass is intersected by thin (usually 40–80 μm) black veins. The veins are composed of a very fine-grained matrix with disseminated tiny (<1 μm) inclusions of sulfide and metal. Clasts of host matter are also embedded in the vein matrix. Vein walls are often lined by solid sulfide-metal mixtures. The sample also contains thicker

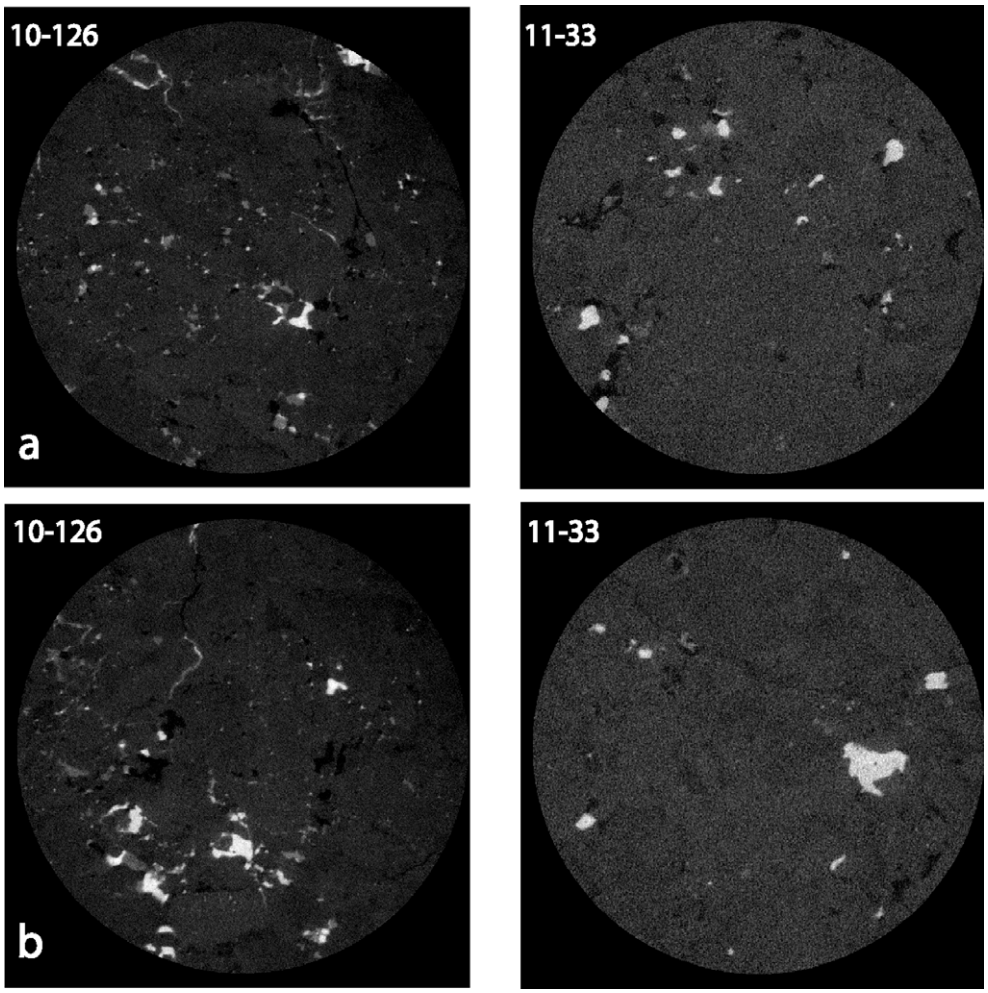

Fig. 14. Microtomographic images (a) and (b) of the "standard" DV sample 10–126 (to the left) and anomalous DV sample 11–33 (to the right). Bright light gray phases correspond to FeNi, while darker gray phases correspond to sulfides.

(0.5–1.5 mm) dikes (or melting zones) that are composed of a very fine-grained silicate matrix with troilite and troilite-metal spherules of 1–5 μm in diameter. The matrix of the dikes comprises a large amount (>50%) of fragmentary minerals, mostly olivine. Sample 10–90 is texturally and structurally indistinguishable from the dark variety of the Chelyabinsk meteorite (Galimov et al. 2013). A particularly noteworthy feature is the presence of a large metallic inclusion 3 × 1.5 mm in size (Figs. 15a–c). This inclusion consists of a taenite core with a troilite shell and a kamacite mantle. An intermediate diffuse taenite zone with lower Ni content occurs between the core and the mantle.

The chemistry of the constituent silicate minerals in sample 10–90 also provides useful information for evaluating its anomalous magnetic behavior. The fayalite (Fa) content in olivine varies from 27.9 to 29.4 wt% and ferrosilite (Fs) and wollastonite (Wo) contents in low-Ca pyroxene occur in ranges of 23.2–24.0 wt% and 1.1–1.6 wt%, respectively. Compositions of olivine and pyroxene from sample 10–90 (Table 4) are very similar to those of LL chondrites and are located in low-Fe region of the Fs-Fa diagram occupied by LL chondrites (Brearly and Jones 1998). These data agree well with previously published data on the olivine and pyroxene compositions of the Chelyabinsk LL5 chondrite (Galimov et al. 2013). Chromite compositions (Table 4) also agree well with expected compositions for LL chromites (Brearly and Jones 1998; Wlotzka 2005). Ilmenite in sample 10–90 displays higher Fe contents compared to H and L chondrites (Brearly and Jones 1998). Furthermore, kamacite and taenite Ni-Co wt ratios also lie in ranges typical for LL chondrites (Afiattalab and Wasson 1980).

Thus, the mineral texture, microstructure, and geochemistry of sample 10–90 indicate that it should be classified as a LL chondrite, similar to the rest of the

Table 4. Average element concentrations (in wt%) of olivine, low-Ca pyroxene, and chromite and a representative microprobe analysis of ilmenite from Chelyabinsk meteorite sample 10–90; all Fe is FeO.

Component	Olivine $n = 10$	Low-Ca pyroxene $n = 10$	Chromite $n = 7$	Ilmenite $n = 2$
SiO_2	37.7	55.2	b.d.	55.2
TiO_2	b.d.	0.23	2.88	0.23
Al_2O_3	b.d.	0.17	6.49	0.17
Cr_2O_3	b.d.	0.13	54.2	0.13
V_2O_3	n.d.	n.d.	0.76	n.d.
FeO	25.9	15.6	32.2	15.6
MnO	0.45	0.46	0.62	0.46
ZnO	n.d.	n.d.	0.24	n.d.
MgO	35.7	27.1	1.80	27.1
CaO	b.d.	0.76	b.d.	0.76
Total	99.8	99.7	99.2	99.7
	$Fa_{28.8}$	$Fs_{23.6}Wo_{1.5}$		
Fe#			90.9	87.5
Cr#			84.9	

n = number or analyses; b.d. = below detection, n.d. = not determined; Fa = fayalite, Fs = ferrosilite; Wo = wollastonite; Fe# = atomic ratio Fe/(Fe+Mg)×100; Cr# = atomic ratio Cr/(Cr+Al) × 100.

Table 5. Representative microprobe analyses (wt%) of kamacite and taenite from the Chelyabinsk meteorite sample 10–90 (DV).

Element	Taenite (1*)	Taenite (2*)	Kamacite (3*)
Fe	60.8	71.3	92.0
Ni	39.0	27.2	6.35
Co	0.56	1.29	2.57
Total	100.4	99.8	101.0

*See Figs. 1 and 15b for the location of measurement points.

DV material in the Chelyabinsk samples. It is not an H-type inclusion in the Chelyabisk meteorite shower as one might speculate from its magnetic susceptibility. Instead, the anomalously high magnetic susceptibility is likely to be due to the presence of the large, polycrystalline metallic inclusion shown in Fig. 15. The origin of this metallic inclusion is unknown, but Rubin (2007) argues that shock processes may form polycrystalline kamacite. For example, low-Ni kamacite may transform into taenite during quenching and coarsen during moderate postshock annealing.

Paleofield Estimates

Our paleofield estimates from the Chelyabinsk meteorite are significantly higher than those previously proposed for the LL ordinary chondrites (0.05–0.5 μT) (Gattacceca and Rochette 2004). Instead, the mean

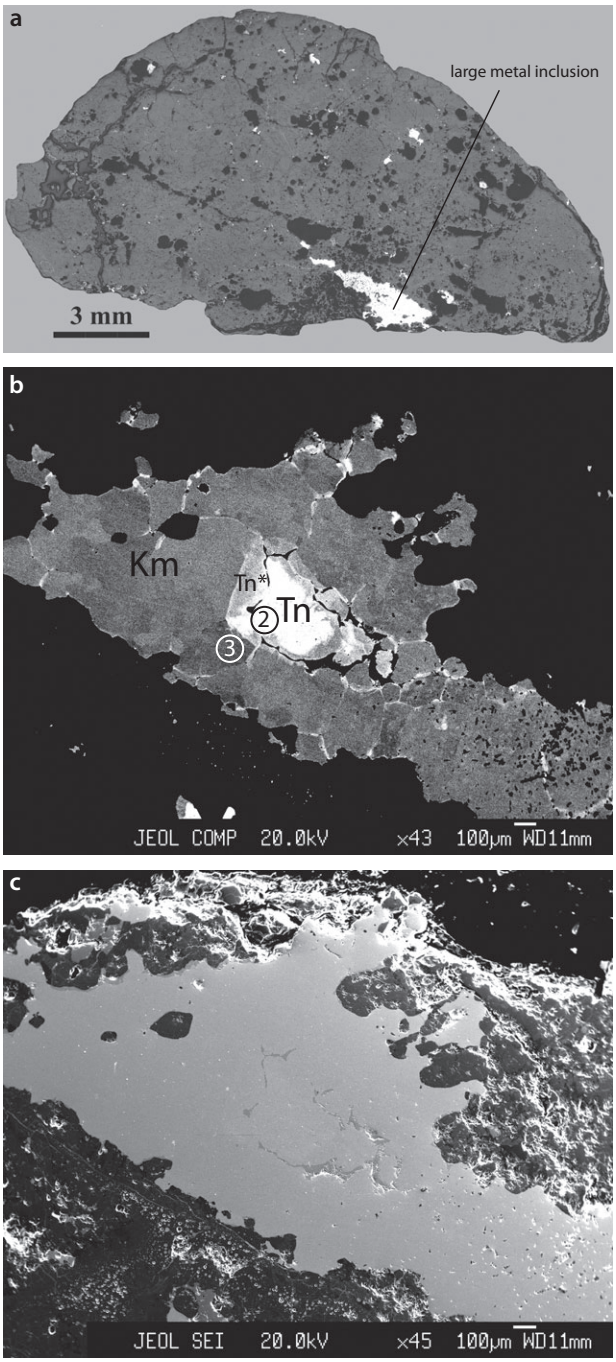

Fig. 15. a) Photomosaic of reflected light microscope images of the sample 10–90. The large metal inclusion is marked by an arrow; b) high contrast backscatter image of the large metal inclusion. The white central taenite (labeled "*Tn*") core is enveloped by sulfide (black) and taenite with lower Ni contents (light gray, labeled "*Tn**"); polycrystalline kamacite grains (gray, labeled "*Km*") have practically identical compositions and their different contrast seems to be due to different crystallographic orientation of the kamacite grains; microprobe data presented in Table 5 (columns 2 and 3 from the left) were collected from the points 2 and 3, which are indicated on the image; c) secondary-electron image of the large metallic inclusion.

paleofield estimates for the LV and DV (18.8 and 16.0 μT, respectively) from the REM method and for the DV (10–50 μT) from the REM′ method are more likely to represent components of a thermoremanent magnetization (TRM) that were acquired as the chondrite was heated and fragmented within the Earth's atmosphere. This is in agreement with the published conclusions of Popova et al. (2013) on the nature of the Chelyabinsk NRM. However, the paleofield estimates of 1138 μT and 1545 μT, suggested by Popova et al. (2013), clearly do not reflect the Earth's magnetic field, and instead, are likely to originate from magnetic contamination of the samples investigated by Popova et al. (2013). Indeed, while their published SIRM value of 1.11×10^{-2} Am^2 kg^{-1} is consistent with our measurements for the LV (see Table 1), their NRM measurement of 3.41×10^{-3} Am^2 kg^{-1} is more than 30 times higher than our mean NRM value for the LV samples. It would be highly unusual for a TRM to be equivalent to >30% of a sample's saturation remanent magnetization.

CONCLUSIONS

1. We measured the low-field magnetic susceptibility of 174 Chelyabinsk fragments from the collection of the Vernadsky Institute (Moscow, Russia) with masses bigger than 3 g. Mean $\log\chi_0$ is 4.57 ± 0.09 (s.d.) ($n = 135$) for the LV and 4.65 ± 0.09 ($n = 39$) (10^{-9} m^3 kg^{-1}) for the DV, indicating that DV is richer in metal. Thus, the Chelyabinsk chondrite does not fall into the standard LL5 range of susceptibility values. Chelyabinsk's χ_0 is three (LV) to four (DV) times higher than the average for LL5 falls, but is similar to a subgroup of other metal-rich LL5 chondrites (Paragould, Aldsworth, Bawku, Richmond), as well as L/LL5 chondrites (Glanerbrug, Knyahinya, Qidong). The average degree of anisotropy is 25%, which agrees with previously published results on LL chondrites of S3 shock stage ($29 \pm 15\%$; Gattacceca et al. 2005).
2. Two Chelyabinsk samples from the Vernadsky collection revealed anomalous magnetic behavior: sample 11–33 (DV) and sample 10–90 (DV) produced $\log\chi_0$ values from H chondrites' range (5.47 and 5.24×10^{-9} m^3 kg^{-1}, respectively). Evidence from X-ray microtomography, petrographic examination, and electron microprobe measurements showed that these two samples are LL chondrites simply enriched in metal and do not represent a separate class of chondrite embedded within the Chelyabinsk meteorite shower.
3. Thermomagnetic analyses indicate that the main magnetic carriers of the Chelyabinsk meteorite at room temperature are populations of taenite and kamacite. In contrast to most other LL chondrites, Chelyabinsk contains no tetrataenite, which suggests that the meteorite experienced a rapid postimpact cooling that disordered any previously existing tetrataenite.
4. Metallic grains of the Chelyabinsk chondrite are largely multidomain with low bulk coercivities B_c (< 1 mT for LV and 1.7 mT for DV) and remanent coercivities B_{cr} (23 mT for LV and 15 mT for DV). FORC diagrams show the distribution of microscopic coercivities extending to higher coercivities: 10 mT for LV and 20 mT for DV. Metallic grains in the DV material are generally on average smaller than those in the LV material and both lithologies contain a significant portion of superparamagnetic grains (< 20 nm in size).
5. Estimation of metal content from M_s values showed that there are 3.7 wt% and 4.1 wt% of metal in the light and dark lithologies, respectively. These M_s-based estimates are favored over estimates based on χ_0, owing to the multitude of physical properties that can influence χ_0 in addition to concentration.
6. At the temperatures < 75 K, chromite becomes ferrimagnetically ordered and acts as an important magnetic remanence carrier. These observations agree with previously published results on ordinary chondrites (Gattacceca et al. 2011).
7. Thermal and alternating field demagnetization spectra for the NRM and SIRM of LV and DV samples are used to apply REM and REM′ paleointensity methods. Most samples did not show any stable components of NRM. However, interpretable NRM records showed a paleofield of the order of approximately 10–50 μT (DV), suggesting that a part of the Chelyabinsk NRM might have been a TRM acquired in the Earth's magnetic field during fragmentation of the Chelyabinsk meteoroid in the terrestrial atmosphere. Previously reported paleofields for LL ordinary chondrites of 0.05 to 0.5 μT (Gattacceca and Rochette 2004) were not observed in the Chelyabinsk chondrite.

Acknowledgments—This research was funded by a U.S. National Science Foundation IRM Visiting Fellowship and the 22nd Program of the Presidium of Russian Academy of Sciences. We acknowledge support from the French X-ray CT platform called Nano-ID, which was funded by the "Investissements d'Avenir" French Government program of the French National Research Agency. We are grateful to Dario Bilardello (IRM), Peter Solheid (IRM), Mike Jackson (IRM) and D.A. Chareev (IEM RAS) for their help and assistance with experiments. We would like to thank Bruce Moskowitz

(IRM) and Subir Banerjee (IRM) for helpful discussions. We thank M. Fuller, C. Suavet, and T. Kohout for their review.

Editorial Handling—Dr. Christian Koeberl

REFERENCES

Acton G., Yin Q.-Z., Verosub K. L., Jovane L., Roth A., Jacobsen B., and Ebel D. S. 2007. Micromagnetic coercivity distributions and interactions in chondrules with implications for paleointensities of the early solar system. *Journal of Geophysical Research* 112:B03S90.

Afiattalab F., and Wasson J. T. 1980. Composition of the metal phases in ordinary chondrites—Implications regarding classification and metamorphism. *Geochimica et Cosmochimica Acta* 44:445–446.

Badyukov D. D., and Dudorov A. E. 2013. Fragments of the Chelyabinsk meteorite shower: Distribution of masses and sizes and constraints on the mass of the largest fragment. *Geochemistry International* 51:583–586.

Banerjee S. K. 1972. Iron-titanium-chromite, a possible new carrier of remanent magnetization in lunar rocks. *Geochimica et Cosmochimica Acta* 3:2337–2342.

Bezaeva N. S., Badjukov D. D., Rochette P., Gattacceca J., Trukhin V. I., Kozlov E. A., and Uehara M. 2010. Experimental shock metamorphism of the L4 ordinary chondrite Saratov induced by spherical shock waves up to 400 GPa. *Meteoritics & Planetary Science* 45:1007–1020.

Bezaeva N. S., Badykov D. D., Nazarov M. A., Rochette P., and Feinberg J. M. 2013. Magnetic properties of the Chelyabinsk meteorite: Preliminary results. *Geochemistry International* 51:568–574.

Borovicka J., Spurny P., Brown P., Weigert P., Kalenda P., Clark D., and Shrbeny L. 2013. The trajectory, structure and origin of the Chelyabinsk asteroidal impactor. *Nature* 503:235–237.

Brearly A. J. and Jones R. H. 1998. Type 4-6 chondrites: Non-opaque material. In *Planetary materials*, edited by Papike J. J. Reviews in Mineralogy, vol. 36. Washington, D.C.: The Mineralogical Society of America. pp. 3-282–3-295.

Chou C.- L., Sears D. W., and Wasson J. T. 1981. Composition and classification of clasts in the St. Mesmin LL chondrite breccia. *Earth and Planetary Science Letters* 54:367–378.

Consolmagno G. J., Macke R. J., Rochette P., Britt D. T., and Gattacceca J. 2006. Density, magnetic susceptibility, and the characterization of ordinary chondrite falls and showers. *Meteoritics & Planetary Science* 41:331–342.

Day R., Fuller M. D., and Schmidt V. A. 1977. Hysteresis properties of titanomagnetites: Grain size and composition dependence. *Physics of the Earth and Planetary Interiors* 13:260–266.

Dunlop D. J. 2002. Theory and application of the Day plot (M_{rs}/M_s versus H_{cr}/H_c) 1. Theoretical curves and tests using titanomagnetite data. *Journal of Geophysical Research* 107:EPM 4-1–EPM 4-22.

Dunn T. L., Cressey G., McSween H. Y., Jr., and McCoy T. J. 2010. Analysis of ordinary chondrites using powder X-ray diffraction: 1. Modal mineral abundances. *Meteoritics & Planetary Science* 45:123–134.

Egli R. 2013. VARIFORC: An optimized protocol for the calculation of non-regular first-order reversal curve (FORC) diagrams. *Global and Planetary Change* 110 (C):302–320.

Galimov E. M., Kolotov V. P., Nazarov M. A., Kostitsyn Y. A, Kubrakova I. V., Kononkova N. N., Roshchina I. A., Alexeev V. A., Kashkarov L. L., Badyukov D. D., and Sevast'yanov V. S. 2013. Analytical results for the material of the Chelyabinsk meteorite. *Geochemistry International* 51:522–539.

Gattacceca J., and Rochette P. 2004. Toward a robust normalized magnetic paleointensity method applied to meteories. *Earth and Planetary Science Letters* 277:377–393.

Gattacceca J., Rochette P., and Bourot-Denise M. 2003. Magnetic properties of a freshly fallen LL ordinary chondrite: The Bensour meteorite. *Physics of the Earth and Planetary Interiors* 140:343–358.

Gattacceca J., Rochette P., Denise M., Consolmagno G., and Folco L. 2005. An impact origin for the foliation of ordinary chondrites. *Earth and Planetary Science Letters* 234:351–368.

Gattacceca J., Rochette P., Gounelle M., and Van Ginneken M. 2008. Magnetic anisotropy of HED and Martian meteorites and implications for the crust of Vesta and Mars. *Earth and Planetary Science Letters* 270:280–289.

Gattacceca J., Bourot-Denise M., and Lenssen R. 2009. NWA 5764: The first LL-L chondrite (abstract #5085). *Meteoritics & Planetary Science* 44:A75.

Gattacceca J., Rochette P., Lagroix F., Mathé P.-E., and Zanda B. 2011. Low temperature magnetic transition of chromite in ordinary chondrites. *Geophysical Research Letters* 38:L10203.

Gattacceca J., Suavet C., Rochette P., Weiss B., Winklhofer M., Uehara M., and Friedrich J. 2014. Metal phases in ordinary chondrites: Magnetic hysteresis properties and implications for thermal history. *Meteoritics & Planetary Science*. 49:652–676, doi:10.1111/maps.12268.

Harrison R. J., and Feinberg J. M. 2008. FORCinel: An improved algorithm for calculating first-order reversal curve (FORC) distributions using locally weighted regression smoothing. *Geochemistry, Geophysics, Geosystems* 9(5): Q05016.

Jarosewich E. 1990. Chemical analyses of meteorites: A compilation of stony and iron meteorite analyses. *Meteoritics* 25:323–337.

Jelinek V. 1978. Statistical processing of anisotropy of magnetic susceptibility measured on groups of specimens. *Studia Geophysica et Geodaetica* 22:50–62.

Kneller E. F., and Luborsky F. E. 1963. Particle size dependence of coercivity and remanence of single-domain particles. *Journal of Applied Physics* 34:656–658.

Kohout T., Jenniskens P., Shaddad M. H., and Haloda J. 2010. Inhomogeneity of asteroid 2008 TC_3 (Almahata Sitta meteorites) revealed through magnetic susceptibility measurements. *Meteoritics & Planetary Science* 45:1778–1788.

Kohout T., Gritsevich M., Grokhovsky V. I., Yakovlev G. A., Haloda J., Halodova P., Michallik R. M., Penttilä A., and Muinonen K. 2014. Mineralogy, reflectance spectra, and physical properties of the Chelyabinsk LL5 chondrite—Insight into shock-induced changes in asteroid regoliths. *Icarus* 228:78–85.

Lappe S.-C. L. L., Feinberg J. M., Muxworthy A., and Harrison R. J. 2013. Comparison and calibration of nonheating paleointensity methods: A case study using

dusty olivine. *Geochemistry, Geophysics, Geosystems* 14: 2143–2158.

Oshtrakh M. I., Petrova E. V., Grokhovsky V. I., and Semionkin V. A. 2008. A study of ordinary chondrites by Mössbauer spectroscopy with high-velocity resolution. *Meteoritics & Planetary Science* 43:941–958.

Oshtrakh M. I., Grokhovsky V. I., Petrova E. V., and Semionkin V. A. 2013. The first results of Mössbauer study of Chelyabinsk LL5 meteorite fragment. *Meteoritics & Planetary Science* 48:A274.

Petrovsky E., and Kapicka A. 2006. On determination of the Curie point from thermomagnetic curves. *Journal of Geophysical Research* 111:B12S27.

Popova O. P., Jenniskens P., Emel'yanenko V., Kartashova A., Biryukov E., Khaibrakhmanov S., Shuvalov V., Rybnov Y., Dudorov A., Grokhovsky V. I., Badyukov D. D., Yin Q.-Z., Gural P. S., Albers J., Granvik M., Evers L. G., Kuiper J., Kharlamov V., Solovyov A., Rusakov Y. S., Korotkiy S., Serdyuk I., Korochantsev A. V., Larionov M. Y., Glazachev D., Mayer A. E., Gisler G., Gladkovsky S. V., Wimpenny J., Sanborn M. E., Yamakawa A., Verosub K. L., Rowland D. J., Roeske S., Botto N. W., Friedrich J. M., Zolensky M. E., Le L., Ross D., Ziegler K., Nakamura T., Ahn I., Lee J. I., Zhou Q., Li X.-H., Li Q.-L., Liu Y., Tang G.-Q., Hiroi T., Sears D., Weinstein I. A., Vokhmintsev A. S., Ishchenko A. V., Schmitt-Kopplin P., Hertkorn N., Nagao K., Haba M. K., Komatsu M., and Mikouchi T. 2013. Chelyabinsk airburst, damage, assessment, meteorite recovery and characterization. *Science* 342:1069–1073.

Rochette P., Sagnotti L., Bourot-Denise M., Consolmagno G., Folco L., Gattacceca J., Osete M. L., and Pesonen L. 2003. Magnetic classification of stony meteorites: 1. Ordinary chondrites. *Meteoritics & Planetary Science* 38:251–268.

Rochette P., Gattacceca J., Bonal L., Bourot-Denise M., Chevrier V., Clerc J.-P., Consolmagno G., Folco L., Gounelle M., Kohout T., Pesonen L., Quirico E., Sagnotti L., and Skripnik A. 2008. Magnetic classification of stony meteorites: 2. Non-ordinary chondrites. *Meteoritics & Planetary Science* 43:959–980.

Rochette P., Gattacceca J., Bezaeva N. S., Obolonskaya E. V., Polyarnaya J. A., Skripnik A. Y., and Nazarov M. A. 2009a. Scanning meteorite collections for misclassified/misidentified samples: Examples from Saint Petersburg and Moscow (abstract #5029). *Meteoritics & Planetary Science* 44:A176.

Rochette P., Gattacceca J., Bourot-Denise M., Consolmagno G., Folco L., Kohout T., Pesonen L., and Sagnotti L. 2009b. Magnetic classification of stony meteorites: 3. Achondrites. *Meteoritics & Planetary Science* 44:405–427.

Rubin A. E. 2007. Petrogenesis of acapulcoites and lodranites: A shock-melting model. *Geochimica et Cosmochimica Acta* 71:2383–2401.

Stöffler D., Keil K., and Scott E. R. D. 1991. Shock metamorphism of ordinary chondrites. *Geochimica et Cosmochimica Acta* 55:3845–3867.

Sugiura N., and Strangway D. W. 1988. Magnetic studies of meteorites. In *Meteoritics and the early solar system*, edited by Kerridge J. E. and Mathews M. S. Tucson, Arizona: The University of Arizona Press. pp. 595–615.

Van de Moortèle B., Reynard B., Rochette P., Jackson M., Beck P., Gillet P., and McMillan P. F. 2007. Shock-induced metallic iron nanoparticles in olivine-rich Martian meteorites. *Earth and Planetary Science Letters* 262:37–49.

Wasilewski P. J. 1982. Magnetic characterization of tetrataenite and its role in the magnetization of meteorites (abstract). 13th Lunar and Planetary Science Conference. p. 843.

Wasilewski P. 1988. Magnetic characterization of the new magnetic mineral tetrataenite and its contrast with isochemical taenite. *Physics of the Earth and Planetary Interiors* 52:150–158.

Weaving B. 1962. Magnetic anisotropy in chondritic meteorites. *Geochimica et Cosmochimica Acta* 26:451–455.

Weiss B. P., Gattacceca J., Stanley S., Rochette P., and Christensen U. R. 2010. Paleomagnetic records of meteorites and early planetesimal differentiation. *Space Science Reviews* 152:341–390.

Wlotzka F. 2005. Cr spinel and chromite as petrogenetic indicators in ordinary chondrites: Equilibration temperatures of petrologic types 3.7 to 6. *Meteoritics & Planetary Science* 40:1673–1702.

Yanai K., and Kojima H. 1993. Regolith breccia consisting of H and LL chondrite mixture (abstract). 24th Lunar and Planetary Science Conference. p. 1553.